DEPARTMENT OF OCEAN ENGINEERING
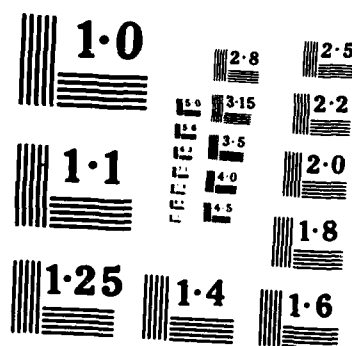
MASSACHUSETTS INSTITUTE OF TECHNOLOGY

CAMBRIDGE, MASSACHUSETTS 02139

PERFORMANCE EVALUATION OF PLATE - FIN

HEAT EXCHANGERS

DY

DAVID MICHAEL CECI

JUNE, 1987

COURSE: XIII-A   COPY NUMBER: 5

PERFORMANCE EVALUATION OF PLATE - FIN HEAT EXCHANGERS

by

DAVID MICHAEL CECI

B.S.M.E., PURDUE UNIVERSITY
(1979)

SUBMITTED IN PARTIAL FULFILLMENT
OF THE REQUIREMENTS FOR THE
DEGREES OF

MASTER OF SCIENCE IN NAVAL ARCHITECTURE AND MARINE
ENGINEERING

and

MASTER OF SCIENCE IN MECHANICAL ENGINEERING

at the

MASSACHUSETTE INSTITUTE OF TECHNOLOGY

JUNE, 1987   *N00228-85-G-3262*

© DAVID MICHAEL CECI

The author hereby grants to M.I.T. and the U.S. Government
permission to reproduce and to distribute copies of this
thesis document in whole or in part.

Signature of Author _____
Department of Ocean Engineering
May, 1987

Certified by _____
Professor Warren M. Rohsenow
Mechanical Engineering Department, Thesis Supervisor

Certified by _____
Professor Paul Sullivan
Ocean Engineering Department, Thesis Reader

Accepted by _____
Professor A. Douglas Carmichael
Chairman, Ocean Engineering Departmental Committee

Accepted by _____
Professor Ain A. Sonin
Chairman, Mechanical Engineering Departmental Committee

PERFORMANCE EVALUATION OF PLATE - FINNED HEAT EXCHANGERS

by

DAVID MICHAEL CECI

ABSTRACT

The performance parameters proposed by Soland et al. [2] was used to perform a comparison of the Kays and London [3] plate - finned surfaces for heat exchangers constructed from stainless steel, mild steel, aluminum, and copper. Three additional comparison criteria were also investigated by modifying the proposed parameters. When using stainless steel, the louvered plate - finned surface 1/4 (b) - 11.1. is the best, but when using mild steel, aluminum, or copper, the wavy - fin plate - finned surface 17.8 - 3/8W is the best of those considered.

Thesis Supervisor: Professor Warren M. Rohsenow
Title: Professor of Mechanical Engineering

ACKNOWLEDGEMENTS

I would like to express my sincere gratitude to Professor Warren M. Rohsenow for his understanding, guidance and patience throughout this work.

I am also deeply indebted to my wife, Venancia, and our children for their support, patience, understanding, and love during the preparation of this thesis and for the period of study at M.I.T.

TABLE OF CONTENTS

NOMENCLATURE

SYMBOL	DEFINITION	UNITS
a	heat exchanger width	ft
A_b	heat transfer area of base surface without enhancement; equals length times heated perimeter	ft^2
A_c	minimum free flow area	ft^2
A_f	frontal area of heat exchanger	ft^2
A_F	flow area without enhancement	ft^2
A_h	total heat transfer area	ft^2
b	plate spacing	ft
c_p	specific heat	BTU/lb_m F
d	pin diameter	ft
D_n	nominal diameter; defined by (1b)	ft
f	friction factor based on total area (A_h); defined by (4a)	- - -
f_n	nominal friction factor based on base area (A_b); defined by (4b)	- - -
f_s	friction factor for a smooth surface; defined by (28)	- - -
g_o	conversion factor (= 32.174)	lb_m ft/lb_f s^2
G_c	mass flux based on minimum free flow area; defined by (2a)	lb_m/hr ft^2
G_n	nominal mass flux based on flow area (A_F); defined by (2b)	lb_m/hr ft^2
h	heat transfer coefficient based on total area (A_h); defined by (5a)	BTU/hr ft^2 F
h_n	nominal heat transfer coefficient based on base area (A_b); defined by (5b)	BTU/hr ft^2 F
J	Colburn J factor based on total area (A_h); defined by (7a)	- - -

J_n	nominal Colburn j factor based on base area (A_b); defined by (7b)	- - -
J_s	Colburn j factor for smooth surface; defined by (26)	- - -
k_m	thermal conductivity of material	BTU/hr ft F
l	fin length from root to center; (= b/2)	ft
L	heat exchanger length	ft
m	fin parameter; defined by (10)	1/ft
Nu	Nusselt number; defined by (6a)	- - -
Nu_n	nominal Nusselt number; defined by (6b)	- - -
NTU	number of heat transfer units; defined by (23)	- - -
P	pumping power	hp
Pr	Prandtl number	- - -
q	heat transfer rate	BTU/hr
4rh	hydraulic diameter; defined by (1a)	ft
Re	Reynolds number based on minimum free flow area (A_c); defined by (3a)	- - -
Re_n	nominal Reynolds number based on free flow area (A_F); defined by (3b)	- - -
T	temperature	F
V	heat exchanger volume on one side	ft^3

MISCELLANEOUS

β	ratio of heat transfer area (A_h) to volume	ft^2/ft^3
ΔP_f	friction pressure drop	lb_f/ft^2
ω	mass flow rate	lb_m/hr
η_f	fin efficiency; defined by (9)	- - -
η_o	total surface efficiency; defined by (8)	- - -
ν	viscosity	$lb_m/hr\ ft$
ρ	density	lb_m/ft^3
ϵ	heat exchanger effectiveness	- - -
δ	fin thickness	ft

SUBSCRIPTS

a	case a parameter	- - -
b	case b parameter	- - -
c	case c parameter	- - -
d	case d parameter	- - -
e	case e parameter	- - -
f	case f parameter	- - -
g	case g parameter	- - -
es	enhanced surface	- - -
s	smooth surface	- - -
n	mominal	- - -

LIST OF FIGURES

LIST OF TABLES

I. INTRODUCTION

Plate - fin surfaces have been used for many years in heat exchanger design. Various attempts have been made to develope a universal comparison method to evaluate the performance of enhanced surfaces. These comparison methods provide ways for the designer to select the most beneficial surface for a given application. Any comparison method should be easy to apply and give accurate results. The most notable of these attempts have been by Bergles et al. [1], Webb [6], Webb et al. [7], LaHaye et al. [8], and Cox et al. [11].

LaHaye et al. [8] proposed a method using an effective uninterrupted flow length to diameter ratio of the surface to determine the relative performance of different heat exchanger surfaces. This comparison method was modified by Soland et al. [2] and used to compare the plate - finned surfaces of Kays and London [3] using aluminum as the heat exchanger material. From these proposed performance parameters four cases could be investigated when the flow rate and inlet temperatures between the surfaces being compared were held constant. The cases were:

    a) Same shape and volume.

    b) Same volume and pumping power.

    c) Same pumping power and number of transfer units.

    d) Same volume and number of transfer units.

Aluminum may not be the best material to use for heat exchanger construction in all applications. Plate spacing, fin thickness, and material thermal conductivity are three of the parameters that determine fin efficiency and subsequently the surface efficiency. These factors prevent the "best" aluminum surface from being the "best" when a different material is used. Here the proposed performance parameters of Soland et al. [2] are used to investigate which surafce is the "best" for four different materials - - stainless steel, mild steel, aluminum, and copper. Their performance parameters are also further modified to investigate three additional cases:

> e) Same shape, volume, and pressure drop.
>
> f) Same frontal area and heat transfer.
>
> g) Same frontal area and pumping power.

II. PERFORMANCE PARAMETERS

Kays and London [3], presents data for many different plate - finned surfaces in terms of Colburn j factors, j, and friction factors, f, as a function of Reynolds number Re. The total heat transfer area of the surface, A_h, is the reference area for j and f while the minimum free flow area, A_c, is the reference for Re.

The proposed comparison method of Soland et al. [2] converts the magnitudes of j and f referenced to the surface base plate area, A_b, to obtain new "nominal" values, j_n and f_n. These values will include the effect on the base plate area of the fins. The new j_n includes the total heat transfer area but is based on the plate area; hence $j_n > j$. Since j is proportional to the local heat transfer coefficient, h, this implies that $h_n > h$. Similarly the new friction factor includes the total friction effect but is based on the plate area as though the fins were not present; also $f_n > f$. Further, since h_n includes the effect of the fins it becomes a function of fin material thermal conductivity. The f_n, however, is independent of fin conductivity. The new "nominal" Reynolds number, Re_n, will be based on the open flow area, A_F, as though the fins were not present.

Table I shows the proposed new definitions of the various quantities compared with the definitions used by Kays and London [3].

Figure 1 shows a representative surface geometry and a sample calculation for the proposed hydraulic diameter, D_n, and mass flux, G_n, of a smooth surface passage and the Kays and London plain plate - fin surface 6.2. Note that $D_n = 2b$ for either a finned or unfinned parallel plate passage.

To convert the Kays and London data to the new basis, the following ratios are obtained from the definitions of Table I and Figure 1.

$$\frac{A_b}{A_h} = \frac{2aL}{\beta V} = \frac{2}{\beta b} \tag{11}$$

where $\beta = A_h/V$

$$\frac{A_F}{A_c} = \frac{abL}{A_h r_h} = \frac{1}{\beta r_h} \tag{12}$$

$$\frac{G_n}{G_c} = \frac{A_c}{A_F} = \beta r_h \tag{13}$$

$$\frac{Re_n}{Re} = \frac{D_n G_n}{4 r_h G_c} = \frac{\beta b}{2} \tag{14}$$

$$\frac{f_n}{f} = \frac{A_F A_h G_c^2}{A_c A_b G_n^2} = \frac{b}{2\beta^2 r_h^3} \tag{15}$$

$$\frac{j_n}{j} = \frac{h_n G_c}{h \, G_n} = \frac{\eta_o b}{2 r_h} \tag{16}$$

These ratios were used to convert Kays and London data to obtain curves of the proposed f_n and j_n as a function of Re_n. To solve for the proper fin efficiency, η_f, two assumptions were required: selection of the heat exchanger material and operating fluid. The gas selected was air at

400 F (c_p = 0.2451 BTU/lb_m F, μ = 0.0624 lb_m/ft hr, Pr = 0.683). Four different heat exchanger materials were analysed; stainless steel (km = 10 BTU/hr ft F), mild steel (km = 25 BTU/hr ft F), aluminum (km = 100 BTU/hr ft F), and copper (km = 225 BTU/hr ft F).

A representative set of curves for the Kays and London plain plate - fin surface 6.2 of reference [3] is shown in Figure 2 for aluminum heat exchanger material.

Using the definitions from Table I, two power performance parameters can be developed. For any heat exchanger, the pumping power required for one side is:

$$P = \frac{w}{\rho} \Delta P_f \qquad (17)$$

Substituting for ΔP_f from equation (4b) and using equation (3b) results in:

$$P = \frac{2\mu^2}{g_o \rho^2} wL \frac{f_n Re_n^2}{D_n^3} \qquad (18)$$

$$P = \frac{3\mu^3}{g_o \rho^2} A_F L \frac{f_n Re_n^3}{D_n^4} \qquad (19)$$

Rearranging equations (18) and (19) gives:

$$\frac{f_n Re_n^2}{D_n^3} = \frac{g_o \rho^2}{2\mu^2} \frac{P}{wL} \qquad (20a)$$

$$= \frac{g_o \rho}{2\mu^2} \frac{\Delta P_f}{L} \qquad (20b)$$

$$\frac{f_n Re_n^3}{D_n^4} = \frac{g_c \rho^2}{2\mu^3} \frac{P}{V}$$

(21)

These two equations are the power performance parameters.

The heat transfer for any heat exchanger is given by:

$$q = \epsilon(T_{h,in} - T_{c,in})wc_p$$ (22a)

$$= A_h h \Delta T_{lm}$$ (22b)

$$= wc_p \Delta T_r$$ (22c)

For any flow arrangement, a curve similar to Figure 3 exists which relates ϵ to NTU, where:

$$NTU = \frac{A_h h}{wc_p}$$ (23)

This relationship between ϵ and NTU is always monotonically increasing. The log mean temperature difference, ΔT_{lm}, is defined by Figure 4 and is applicable to all single pass flow arrangements except for cross flow heat exchangers. In a cross flow exchanger ΔT_{lm} must be corrected as described in reference [4].

Heat transfer performance parameters can be developed from the definitions, (3b) and (7b) of Table I and equations (22) and (23) resulting in the following:

$$\frac{j_n}{D_n} = \frac{P_r^{2/3}}{4wc_p} \frac{A_h h_n}{L}$$ (24a)

$$= \frac{P_r^{2/3}}{4wc_p} \frac{q}{\Delta T_{lm} L}$$ (24b)

$$= \frac{P_r^{2/3}}{4L} \, NTU \qquad (24c)$$

$$= \frac{P_r^{2/3}}{4L} \, \ln \frac{\Delta T_1}{\Delta T_o} \qquad (24d)$$

$$\frac{J_n Re_n}{D_n^2} = \frac{P_r^{2/3}}{4\mu c_p} \frac{A_h h_n}{V} \qquad (25a)$$

$$= \frac{P_r^{2/3}}{4\mu c_p} \frac{q}{\Delta T_{1m} V} \qquad (25b)$$

$$= \frac{P_r^{2/3}}{2\mu} \, \omega \, \frac{NTU}{V} \qquad (25c)$$

Equations (24) and (25) are the heat transfer performance
parameters.

With the surface data in the form of J_n and f_n as a
function of Re_n, the performance parameters can be
constructed into performance curves and plotted. A different
curve will result for each surface.

Since J_n/D_n and $f_n Re_n^2/D_n^3$ have a common heat exchanger
dimension of length, they will be used to generate one set
of performance curves. Volume is the common dimension for
$J_n Re_n/D_n^2$ and $f_n Re_n^3/D_n^4$ so they will be used together to
generate another set of performance curves.

Figure 5 shows representative performance curves for two
Kays and London surfaces when plotted as J_n/D_n as a function
of $f_n Re_n^2/D_n^3$. Figure 6 shows the same two surfaces for the
other performance parameters, $J_n Re_n/D_n^2$ and $f_n Re_n^3/D_n^4$. In
both figures, Re_n can be represented as shown.

TABLE I: DEFINITIONS

Quantity	Kays & London [3]		Proposed	
hydraulic diameter	$4r_h = \dfrac{A_c\,L}{A_h}$	(1a)	$D_n = \dfrac{4A_F L}{A_b} = \dfrac{4V}{A_b}$	(1b)
mass flux	$G_c = \dfrac{w}{A_c}$	(2a)	$G_n = \dfrac{w}{A_F}$	(2b)
Reynolds number	$Re = \dfrac{G_c\,4r_h}{\mu}$	(3a)	$Re_n = \dfrac{G_n\,D_n}{\mu}$	(3b)
friction factor	$f = \dfrac{\Delta P_f}{\dfrac{L}{r_h}\dfrac{G_c^2}{2\rho g_o}}$	(4a)	$f_n = \dfrac{\Delta P_f}{4\dfrac{L}{D_n}\dfrac{G_n^2}{2\rho g_o}}$	(4b)
heat transfer coefficient	$h = \dfrac{q/\eta_o\,A_h}{\Delta T}$	(5a)	$h_n = \dfrac{q/A_b}{\Delta T}$	(5b)
Nusselt number	$Nu = \dfrac{4r_h\,h}{k}$	(6a)	$Nu_n = \dfrac{h_n\,D_n}{k}$	(6b)
Colburn J factor	$j = \dfrac{h\,Pr^{2/3}}{G_c\,c_p}$	(7a)	$j_n = \dfrac{h_n\,Pr^{2/3}}{G_n\,c_p}$	(7b)
Surface efficiency	$\eta_o = 1 - \dfrac{A_f}{A_h}(1 - \eta_f)$	(8)		
Fin efficiency	$\eta_f = \dfrac{\tanh\,ml}{ml}$	(9)		
Fin parameter	$m = \sqrt{\dfrac{2\,h}{\delta\,k_m}}$	(10a)	thin sheet fins	
	$m = \sqrt{\dfrac{4\,h}{d\,k_m}}$	(10b)	circular pin fins	

a) Smooth Surface Passage

$A_F = ab$

$A_b = 2aL$

$V = abL$

$D_n = 4 \dfrac{V}{A_b} = 4 \dfrac{abL}{2aL} = 2b$

$G_n = \dfrac{\omega}{A_F} = \dfrac{\omega}{ab}$
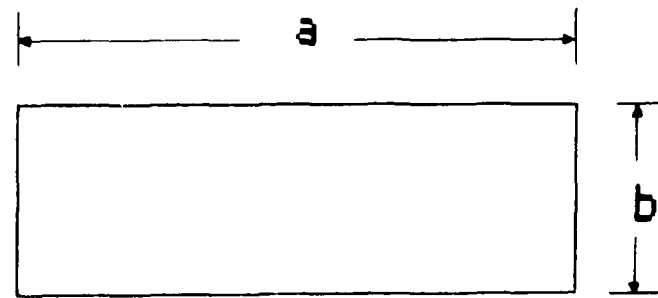
b) Plain Plate - Fin Surface 6.2

$A_F = ab$

$A_b = 2aL$

$V = abL$

$D_n = 4 \dfrac{V}{A_b} = 4 \dfrac{abL}{2aL} = 2b$

$G_n = \dfrac{\omega}{A_F} = \dfrac{\omega}{ab}$
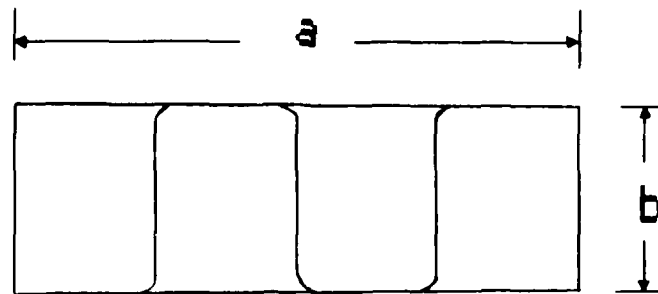
Figure 1: Sample Calculation of Nominal Diameter and Mass Flux for Rectangular Flow Passages.
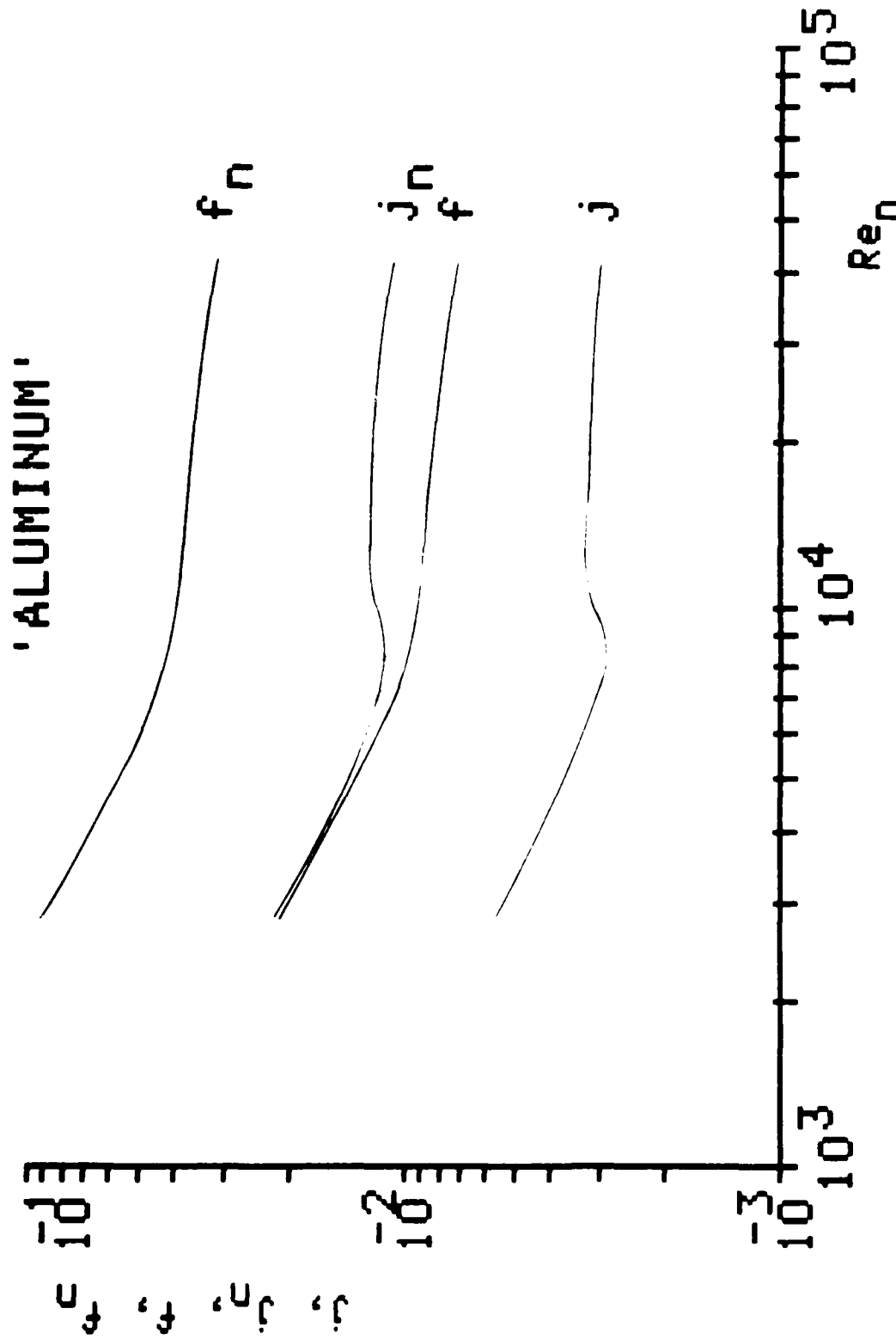
Figure 2: Colburn j-Factors (j, j_n) and Friction Factors (f, f_n) for Plain Plate - Fin Surface 6.2.
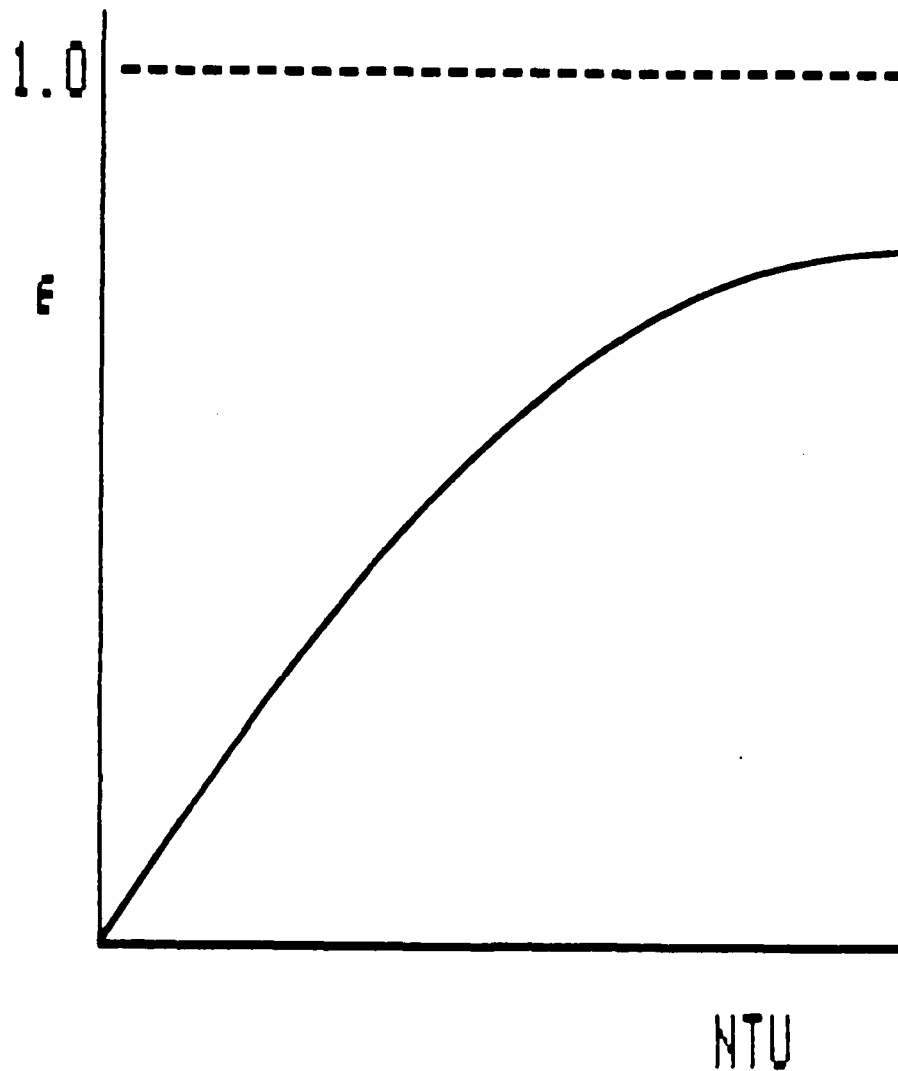
Figure 3: Representative Plot of Heat Exchanger Effectiveness, ε, vs. Number of Transfer Units, NTU.
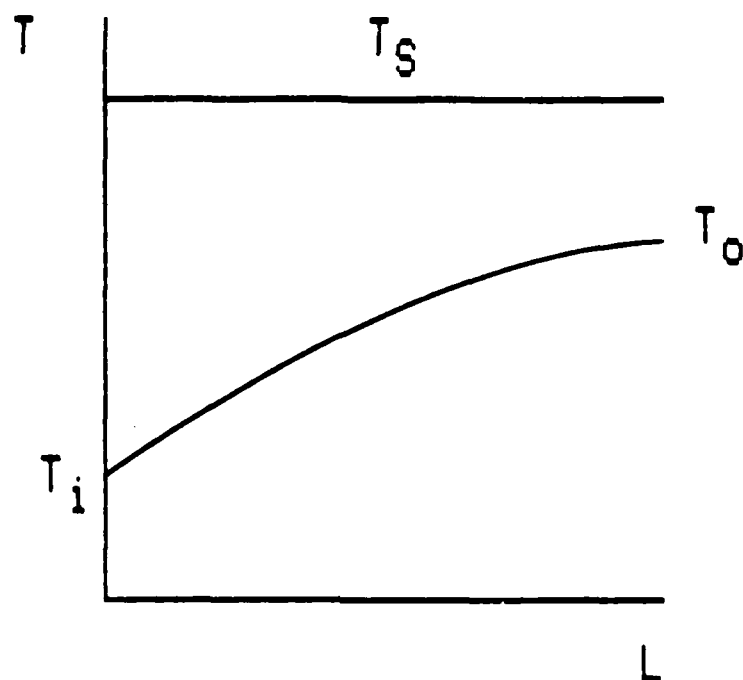
$$\Delta T_i = T_s - T_i \qquad\qquad \Delta T_o = T_s - T_o$$

$$\Delta T_r = T_o - T_i$$

$$\Delta T_{lm} = \frac{\Delta T_i - \Delta T_o}{\ln \dfrac{\Delta T_i}{\Delta T_o}} = \frac{\Delta T_r}{\ln \dfrac{\Delta T_i}{\Delta T_i - \Delta T_r}}$$

Figure 4:   Typical Axial Temperature Distribution for a
Condensor and the Definition of Log Mean
Temperature Difference, ΔT_{lm} .
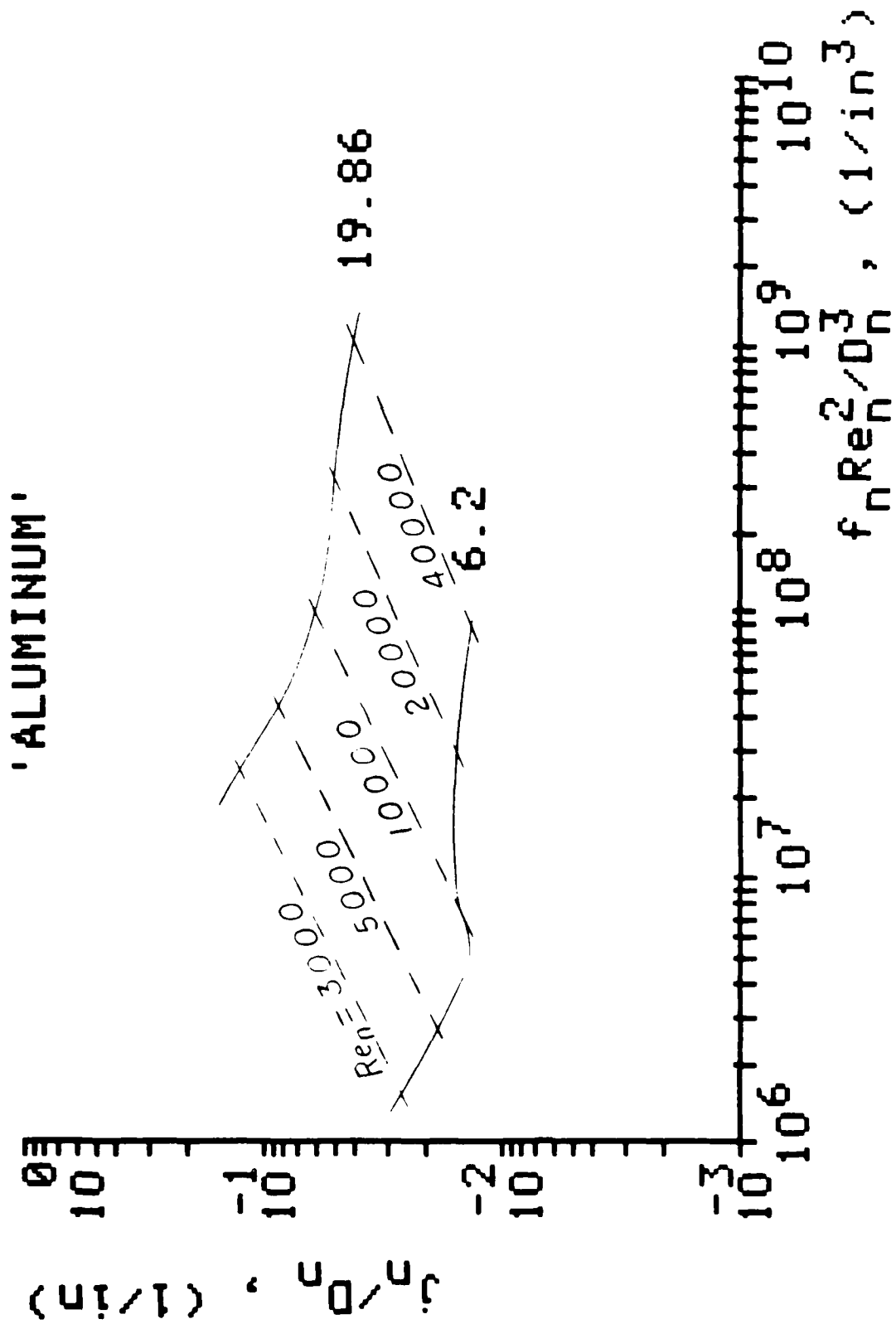
Figure 9. Performance curves for Plain Plate - Fin Surfaces
j_n/D_n and 19.86 for j_n/D_n and $f_n Re_n^2/D_n^3$.
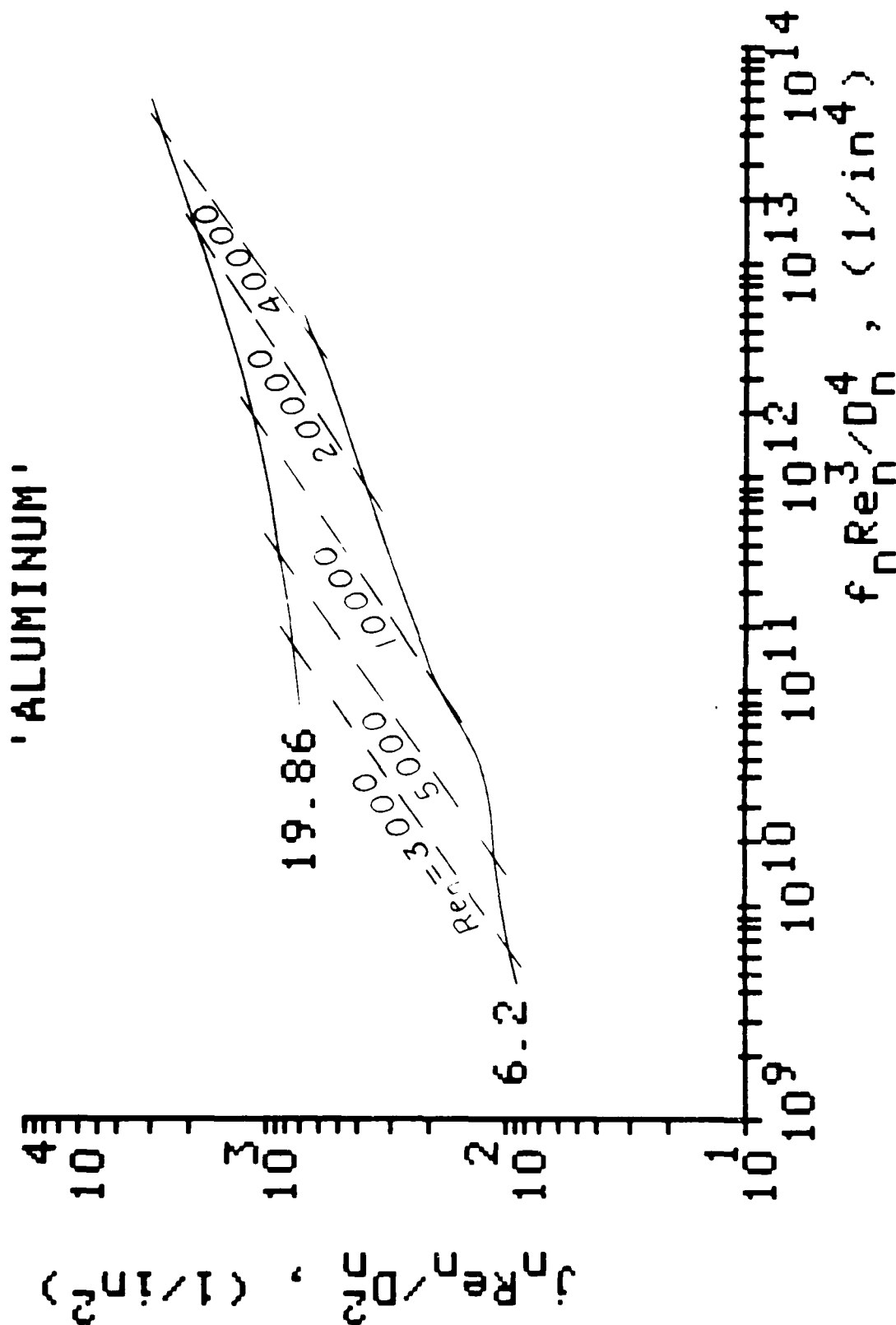
Figure 6: Performance Curves for Plain Plate - Fin Surfaces
6.2 and 19.86 for $j_n Re_n/D_n^2$ and $f_n Re_n^3/D_n^4$.

III. COMPARISON METHOD

Consider a heat exchanger with the controlling heat transfer resistance on one side, such as the gas flow side of a condensor or evaporator. This allows the comparison to be conducted on only one side of a plate - finned heat exchanger. The plate resistance separating the two sides of the heat exchanger will be considered negligible, and the heat exchanger inlet temperatures, $T_{h,in}$ and $T_{c,in}$, will remain constant for all cases considered.

Using the two sets of performance parameters (equations (20) and (24), and equations (21) and (25)), seven different cases can be considered. The first four cases were developed by Soland et al. [2] and uses the performance parameters in the form of equations (21) and (25). These cases will be briefly presented for completeness of discussion. The last three cases use the performance parameters in the form of equations (20) and (24).

The two surfaces represented in Figure 7 for the performance parameters of equations (21) and (25) will be used to demonstrate the use of these curves to determine heat exchanger relative performance for the first four cases. These comparisons will be made for the same flow rate and inlet temperatures. This implies that any comparison which results in the same value for NTU/V will also have the same q/V.

Refering to Figure 7, point o on surface 1 represents a reference heat exchanger with the following specifications: P_o, NTU_o, q_o, L_o, $A_{F,o}$, V_o. This point may lie anywhere on the surface 1 performance curve. Points a, b, c, and d on surface 2, represent the four different performance comparisons of Soland et al. [2].

The two surfaces shown in Figure 8 for the performance parameters of equations (20) and (24) will be used to demonstrate their use to determine heat exchanger performance for the last three cases.

Point o in Figure 8 represents the same reference heat exchanger as the previous four cases. For these performance parameters the specifications at point o will be: $\Delta P_{F,o}$, P_o, NTU_o, q_o, $A_{F,o}$, L_o. This point may lie anywhere on the surface 1 performance curve. Points e, f, and g on surface 2 represent the last three performance comparisons.
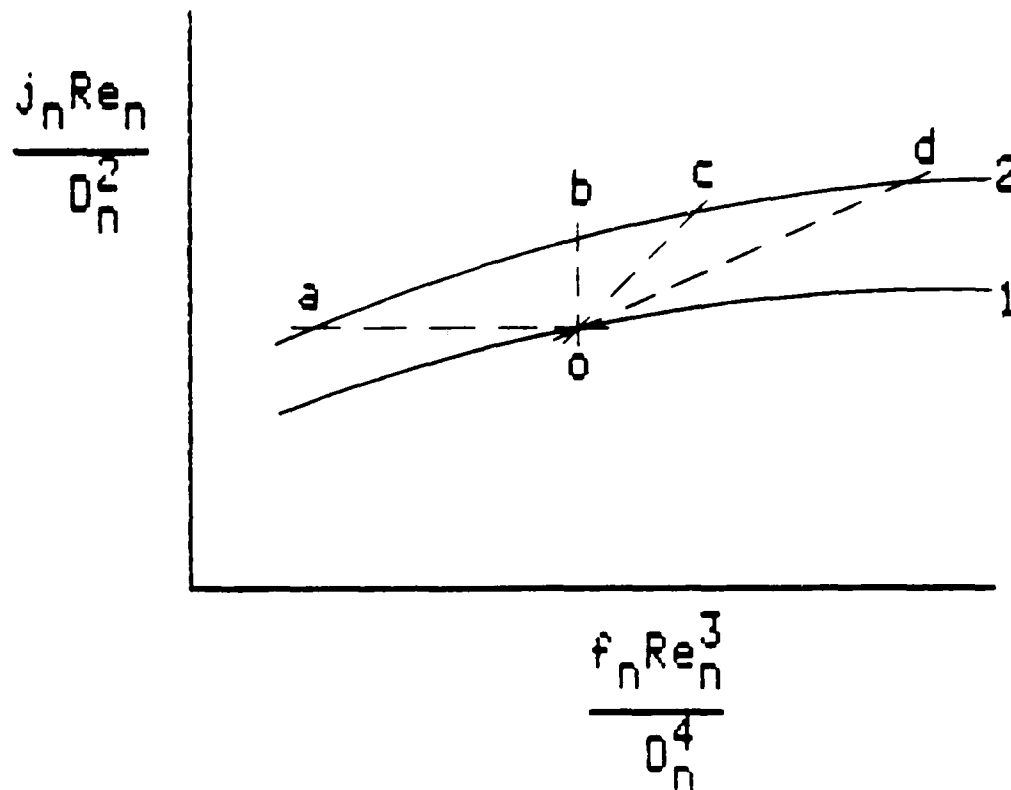
Figure 7:   Representative Performance Curves for Two
Surfaces Showing Points Used for Cases a, b, c,
and d.
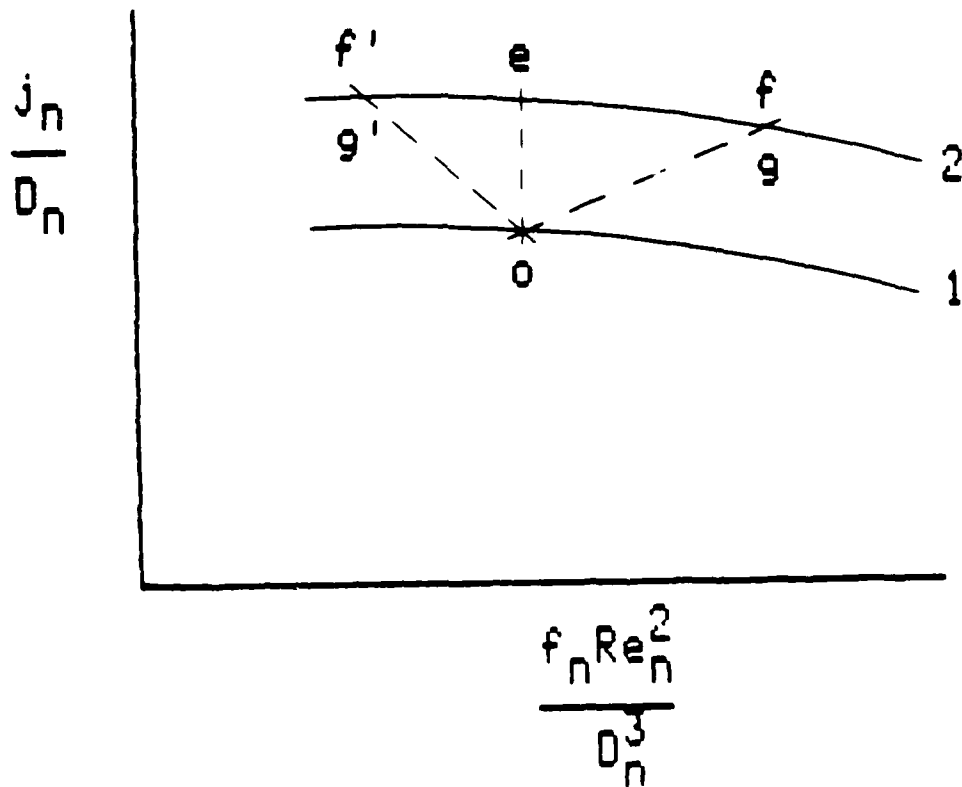
Figure 8: Representative Performance Curves for Two
Surfaces Showing Points Used for Cases e, f, and
g.

Case a:

Same heat exchanger shape, volume, flow rate, and inlet temperatures.

$$L_a = L_o \qquad\qquad w_o = w_o$$

$$A_{F,a} = A_{F,o} \qquad\qquad \Delta T_{i,a} = \Delta T_{i,o}$$

$$V_a = V_o$$

This case represents a comparison of points o and a of Figure 7 by equations (2b) and (3b). The ratios of the ordinate values, equation (25c), and the abscissa values, equation (21), provide the relative changes of heat transfer and pumping power between the two heat exchangers. The necessary ratios are:

$$\frac{Re_{n,a}}{Re_{n,o}} = \frac{D_{n,a}}{D_{n,o}}$$

$$\frac{P_a}{P_o} = \frac{(f_n Re_n^3 / D_n^4)_a}{(f_n Re_n^3 / D_n^4)_o}$$

$$\frac{NTU_a}{NTU_o} = \frac{(j_n Re_n / D_n^2)_a}{(j_n Re_n / D_n^2)_o}$$

Figure 9a shows the magnitude of the increase in pumping power and heat transfer when using surface 2 instead of surface 1 in the same shape and volume heat exchanger.

Case b:

Same heat exchanger volume, pumping power, flow rate, and inlet temperatures.

$$V_b = V_o \qquad w_b = w_o$$

$$P_b = P_o \qquad \Delta T_{i,b} = \Delta T_{i,o}$$

A vertical line on the performance plot of Figure 7 has a fixed value of power per unit volume, equation (21), and is represented by a comparison of points o and b. From equation (25c), the ratio of the ordinate values will yield the number of heat transfer units ratio of the two heat exchangers. The required ratios are:

$$\frac{Re_{n,b}}{Re_{n,o}} = \frac{A_{F,o}}{A_{F,b}} \frac{D_{n,b}}{D_{n,o}}$$

$$\frac{NTU_b}{NTU_o} = \frac{(j_n Re_n / D_n^2)_b}{(j_n Re_n / D_n^2)_o}$$

The magnitude of the increase in heat transfer for the same pumping power when using surface 2 instead of surface 1 is represented in Figure 9b. Note that $Re_{n,b} < Re_{n,o}$ since surface 2 has greater friction than surface 1. If the plate spacing for both surfaces is the same $(D_{n,b} = D_{n,o})$, then the frontal area for surface 2 will be greater than for surface 1, $A_{F,b} > A_{F,o}$. Requiring the same volume means that the length will decrease, $L_b < L_o$.

Case c:

Same heat exchanger pumping power, heat transfer, flow rate, and inlet temperatures.

$$P_c = P_o \qquad\qquad w_c = w_o$$

$$NTU_c = NTU_o \qquad\qquad \Delta T_{i,c} = \Delta T_{i,o}$$

Dividing equation (25c) by equation (21) will result in an equation for a straight line with a unity slope. A line having a slope of 1 in Figure 7 from point o on surface 1 to intersect surface 2 at point c will provide a comparison of required heat exchanger size for the same pumping power and heat transfer rate. Since each axis is inversely proportional to volume, the ratio of either the ordinates or abscissas at points o and c will result in the required heat exchanger volume. The ratios are:

$$\frac{Re_{n,c}}{Re_{n,o}} = \frac{A_{F,o}}{A_{F,c}} \frac{D_{n,c}}{D_{n,o}}$$

$$\frac{V_c}{V_o} = \frac{(f_n Re_n^3/D_n^4)_o}{(f_n Re_n^3/D_n^4)_c} = \frac{(j_n Re_n/D_n^2)_o}{(j_n Re_n/D_n^2)_c}$$

Figure 9c shows the relative reduction in heat exchanger volume when using surface 2 with respect to surface 1. As long as surface 2 lies above surface 1 on the performance curves, surface 2 will result in a smaller heat exchanger volume.

Case d:

Same heat exchanger volume, heat transfer, flow rate,
and inlet temperatures.

$$V_d = V_o \qquad w_d = w_o$$
$$NTU_d = NTU_o \qquad \Delta T_{i,d} = \Delta T_{i,o}$$

A horizontal line on Figure 7 has a constant value of
heat transfer per unit volume; equations (25b) and (25c).
When both heat exchangers have the same overall heat
transfer performance, the ratio of points o and d abscissa
values, equation (21), will provide the pumping power
required by surface 2 compared to surface 1. The ratios are:

$$\frac{Re_{n,d}}{Re_{n,o}} = \frac{A_{F,o}}{A_{F,d}} \frac{D_{n,d}}{D_{n,o}}$$

$$\frac{P_d}{P_o} = \frac{(f_n Re_n^3 / D_n^4)_d}{(f_n Re_n^3 / D_n^4)_o}$$

Figure 9d shows representative results for this
comparison. Note that $Re_{n,d} > Re_{n,o}$. When the plate spacing
for surface 1 and surface 2 are the same ($D_{n,d} = D_{n,o}$), the
frontal area for surface 2 will be greater than surface 1,
$A_{F,d} > A_{F,o}$. The same heat exchanger volume implies that the
length will decrease, $L_d < L_o$. Since $Re_{n,d}$ is the smallest
of these four cases, the frontal area for surface 2 will be
the largest for case d, $A_{F,d} > A_{F,c} > A_{F,b} > A_{F,a}$.

a) **Case a:** Same Shape and Volume
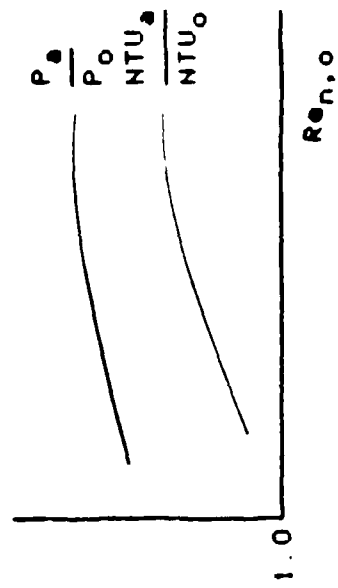
b) **Case b:** Same Power and Volume
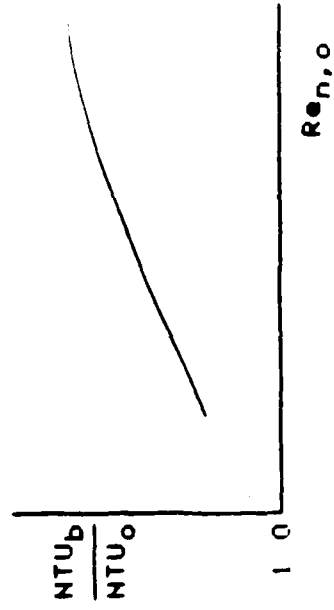
c) **Case c:** Same Power and Heat Transfer

d) **Case d:** Same Volume and Heat Transfer
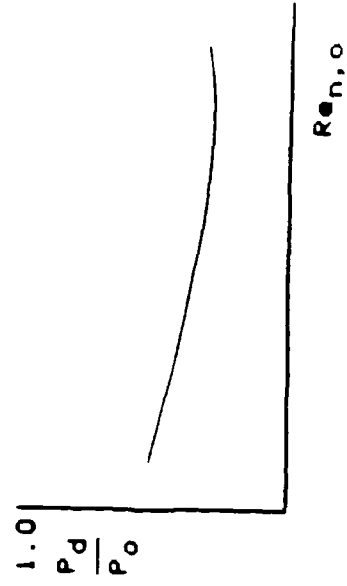
Figure 7. Typical Performance Comparison Results for Case a, b, c, and d.

<u>Case e</u>:

Same heat exchanger shape, volume, pressure drop, and inlet temperatures.

$$L_e = L_o \qquad\qquad \Delta P_{f,e} = \Delta P_{f,o}$$

$$A_{F,e} = A_{F,o} \qquad\qquad \Delta T_{1,e} = \Delta T_{1,o}$$

$$V_e = V_o$$

This case represents a comparison of points o and e of Figure 8 since a vertical line has a fixed value of pressure drop per unit length as shown by equation (20b). Taking ratios of the ordinate values, equatio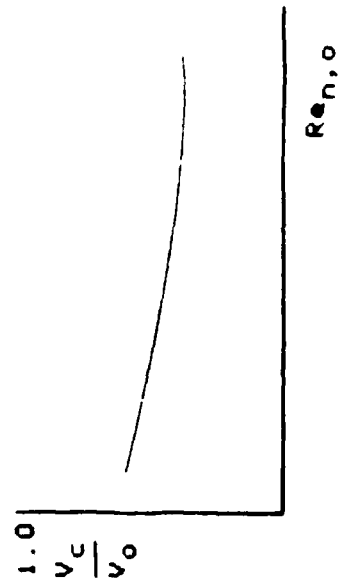n (24c), provides the change in the number of heat transfer units between the two surfaces. The ratio of nominal Reynolds numbers from equations (2b) and (3b) provides the flow rate ratio which will also be equal to the pumping power ratio of the surfaces by equation (20a). Using equation (24c) and (24a) and the temperature definitions from Figure 4, a ratio of the temperature rise for surface 2, $\Delta T_{r,e}$, to the inlet temperatue, ΔT_i , can be determined. This temperature ratio will be a family of curves determined by the selected temperature rise ratio of surface 1. Knowledge of both the temperature rise ratio and flow rate ratio enables a comparison of the heat transfer rates between the two surfaces by use of equation (22c). A family of curves for the heat transfer ratio will also result due to the temperature rise ratio of surface 1. The following ratios are applicable:

$$\frac{\omega_e}{\omega_o} = \frac{Re_{n,e}}{Re_{n,o}} \frac{D_{n,o}}{D_{n,e}} = \frac{P_e}{P_o}$$

$$\frac{NTU_e}{NTU_o} = \frac{(j_n/D_n)_e}{(j_n/D_n)_o}$$

$$\frac{\Delta T_{r,e}}{\Delta T_i} = 1 - (1 - \frac{\Delta T_{r,o}}{\Delta T_i})^{NTU_e/NTU_o}$$

$$\frac{q_e}{q_o} = \frac{\omega_e}{\omega_o} \frac{\Delta T_{r,e}}{\Delta T_i} \frac{\Delta T_i}{\Delta T_{r,o}}$$

Typical results of this comparison are illustrated in Figure 10. A vertical movement on the performance curve between two surfaces results in the upper surface having a smaller nominal Reynolds number, $Re_{n,e} < Re_{n,o}$. If the plate spacing for both surfaces are equal, $D_{n,e} = D_{n,o}$, and since the frontal areas are the same, surface 2 will have a smaller mass flow rate, $\omega_e < \omega_o$. Pumping power is proportional to the product of mass flow rate and pressure drop. This results in a lower pumping power for surface 2, $P_e < P_o$.

The number of heat transfer units for surface 2 is greater than for surface 1, $NTU_e > NTU_o$. However, this does not mean surface 2 will have a greater heat transfer rate than surface 1. Refering to Figure 3, the NTU ratio is seen to be proportional to the surface effectiveness ratio within a constant. Thus, surface 2 is a more effective surface than surface 1. From equations (22a) and (22c) the temperature rise to inlet temperature ratio, $\Delta T_{r,e}/\Delta T_i$, is the surface effectiveness. Surface 1 effectiveness will increase as the temperature ratio increases. Since effectiveness approaches

unity exponentially, the change in the temperature rise for surface 2 becomes less. The combination of reduced flow rate and the interrelationships between NTU, effectiveness, and temperature, can cause a heat transfer ratio less than one.

The above discussion was based on equal plate spacings. If the plate spacing for surface 2 is greater than surface 1, $D_{n,e} > D_{n,o}$, then the hydraulic diameter ratio will be less than unity and the flow rate and pumping power ratios will be smaller. The temperature ratios will not change since they are a function of the NTU ratio. The heat transfer ratio will be less due to the smaller flow rate ratio. If the plate spacing for surface 2 is less than surface 1, $D_{n,e} < D_{n,o}$, then the flow rate and pumping power ratios may be greater than unity. This would increase the heat transfer ratio without any change in the temperature ratios.

Note from Figure 10 however, that there is some combination of parameters that will provide an improved heat transfer for a lower pumping power.
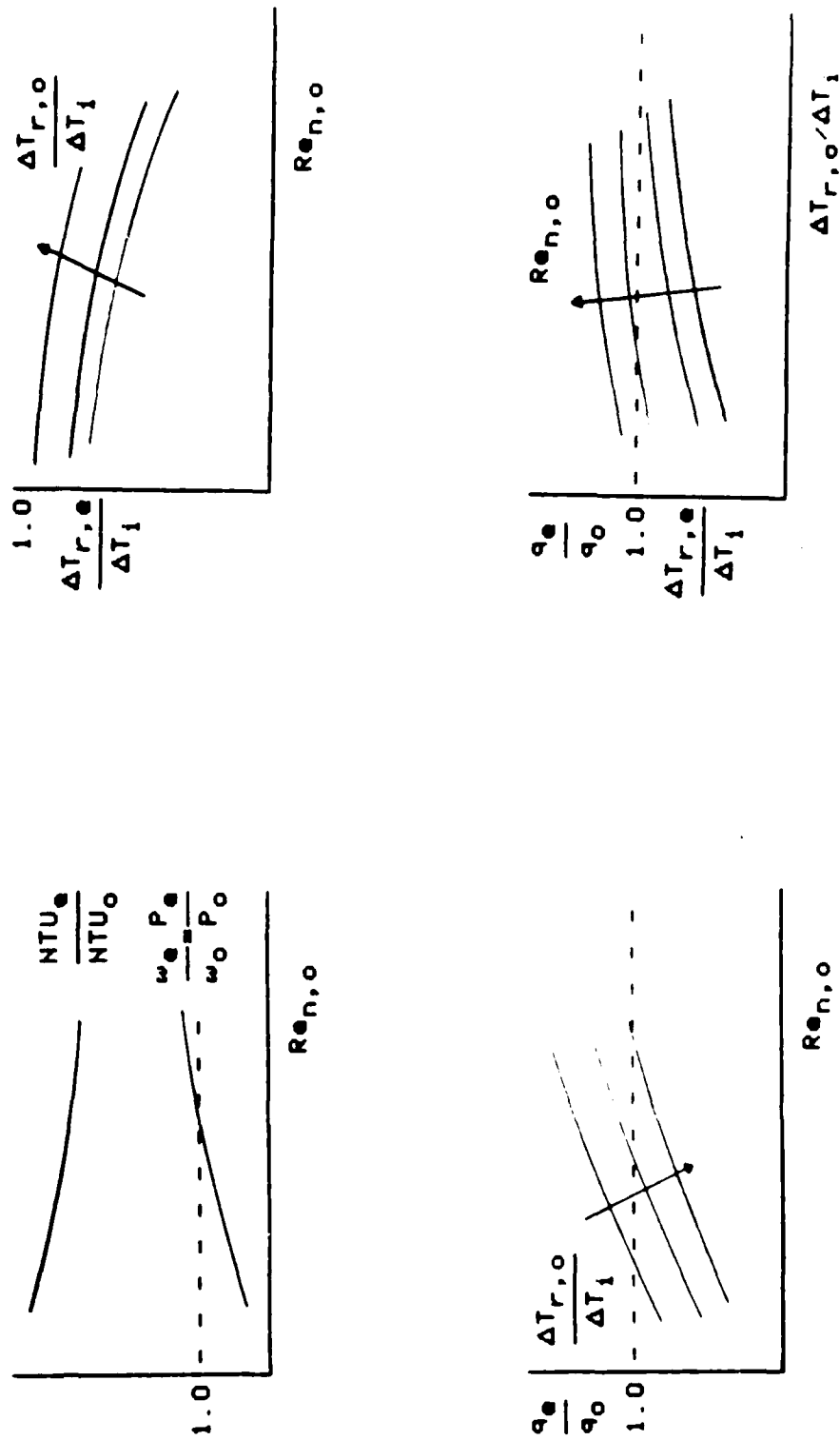
Figure 16. Typical Performance Comparison Results for Case

Case f:

Same heat exchanger frontal area, heat transfer rate, flow rate, and inlet temperatures.

$$A_{F,f} = A_{F,o} \qquad w_f = w_o$$

$$q_f = q_o \qquad \Delta T_{i,f} = \Delta T_{i,o}$$

Using the Reynolds number ratio obtained from equations (2b) and (2c) results in a comparison of points o and f in Figure 8. Since the heat transfer rate and flow rate are the same, the temperature rise across the heat exchanger remains constant and the temperature difference of the outlet is constant, equation (22c). Therefore, from equations (24c) and (24d), NTU remains fixed which means the length ratio of the surfaces can be found from the inverse ratio of the ordinate values. The pumping power ratio, equation (20a), is determined from the product of the abscissa values and the length ratio. The required ratios are:

$$\frac{Re_{n,f}}{Re_{n,o}} = \frac{D_{n,f}}{D_{n,o}}$$

$$\frac{L_f}{L_o} = \frac{(j_n/D_n)_o}{(j_n/D_n)_f}$$

$$\frac{P_f}{P_o} = \frac{(f_n Re_n^2/D_n^3)_f}{(f_n Re_n^2/D_n^3)_o} \frac{L_f}{L_o}$$

Results of the ratios obtained are shown in Figure 11. If the plate spacings of the two surfaces are equal, $D_{n,f} = D_{n,o}$, then the nominal Reynolds numbers are equal, $Re_{n,f} = Re_{n,o}$. Surface 2 is above surface 1 on the performance curve plot because it has greater heat transfer enhancement and

friction. For the same heat transfer rate, the greater heat transfer enhanced surface will require less length, $L_f < L_o$, for the same frontal area - - a smaller heat exchanger. Due to the higher friction of surface 2, it will require more pumping power, $P_f > P_o$. The magnitude of the increase in pumping power is reduced by the decreased length.

The above discussion was based on equal plate spacings. If the plate spacing for surface 2 is greater than surface 1, $D_{n,f} > D_{n,o}$, then the nominal Reynolds number of surface 2 is greater than surface 1, $Re_{n,f} > Re_{n,o}$, and point f moves further to the right on Figure 8. A situation could be reached where the resulting length ratio will be greater than unity. This would occur when the ordinate value of surface 2 becomes less than surface 1. This would require surface 2 pumping power to be greater. If the plate spacings are such that surface 2 is less than surface 1, $D_{n,f} < D_{n,o}$, then the Reynolds number of surface 2 is less than surface 1, $Re_{n,f} < Re_{n,o}$, and point f will move to a point such as f' in Figure 8. In this situation the length ratio will remain less than unity but the pumping power ratio will become less than unity. This is because the abscissa value for surface 2 is less than surface 1.

The results of Figure 11 indicate that for some combination of surface parameters a heat exchanger can be found to provide a shorter length with less pumping power for the same heat transfer, frontal area, and flow rate.
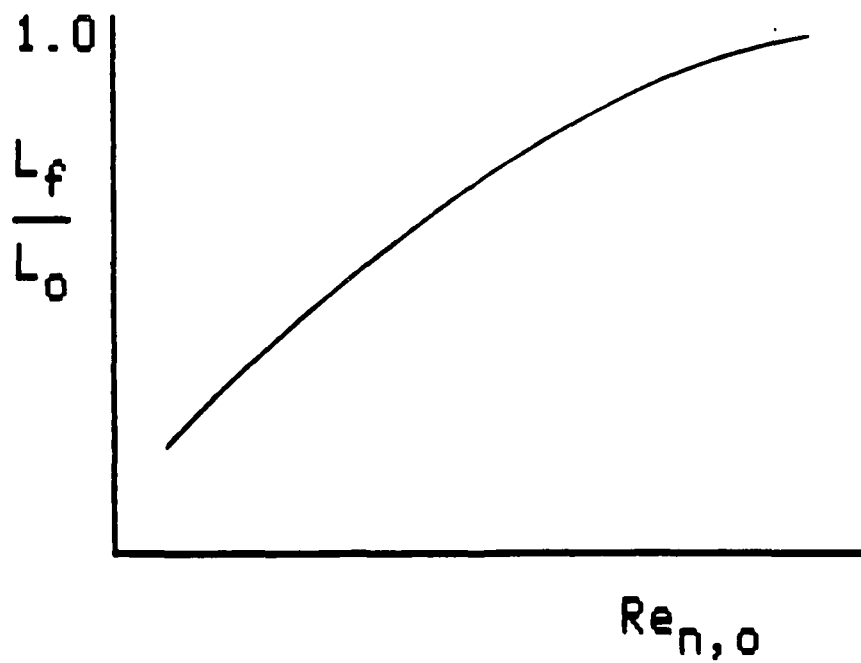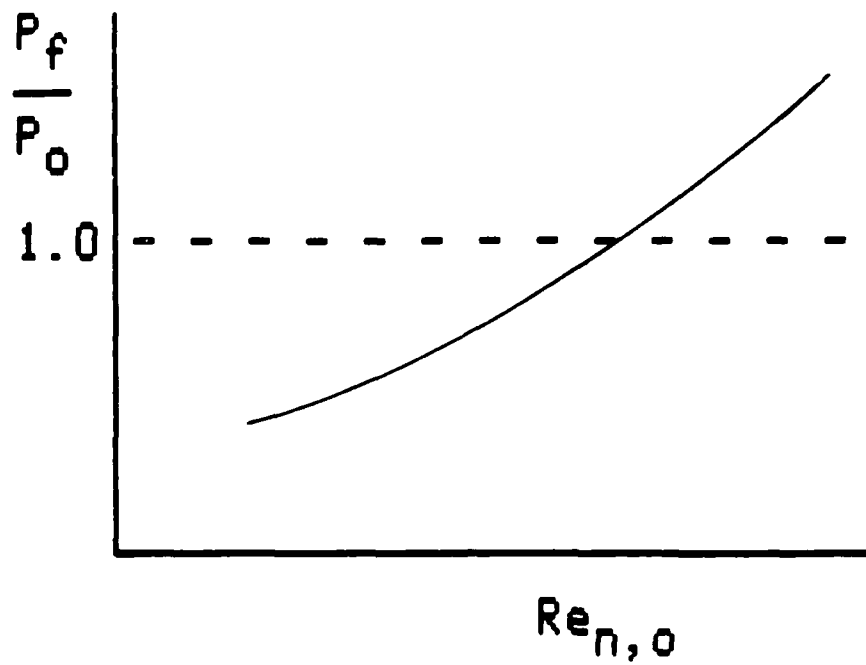
Figure 11: Typical Performance Comparison Results for Case
t.

Case g:

Same heat exchanger frontal area, pumping power, flow rate, and inlet temperatures.

$$A_{F,g} = A_{F,o} \qquad w_g = w_o$$

$$P_g = P_o \qquad \Delta T_{1,g} = \Delta T_{1,o}$$

Points o and g, which are found from the Reynolds number ratio of equations (2b) and (3b), in Figure 8 are indicative of this case. Since pumping power and flow rate are constant, the inverse ratio of the abscissa values will provide the heat exchanger length ratio by equation (20a). The NTU ratio is obtained from the product of the ordinate ratio and the length ratio from equation (24c). As presented for case e, a ratio of the temperature rise for surface 2 to the inlet temperature, $\Delta T_{r,g}/\Delta T_1$, can be determined from equations (24c) and (24d) and Figure 4. This temperature rise ratio will result in a family of curves determined by the selected temperature rise ratio of surface 1. Knowledge of the temperature ratios provides a comparison of the heat transfer rates. A family of curves again result due to the temperature ratios. The ratios are:

$$\frac{Re_{n,g}}{Re_{n,o}} = \frac{D_{n,g}}{D_{n,o}}$$

$$\frac{L_g}{L_o} = \frac{(f_n Re_n^2/D_n^3)_o}{(f_n Re_n^2/D_n^3)_g}$$

$$\frac{NTU_g}{NTU_o} = \frac{(J_n/D_n)_g}{(J_n/D_n)_o} \frac{L_g}{L_o}$$

$$\frac{\Delta T_{r,g}}{\Delta T_1} = 1 - (1 - \frac{\Delta T_{r,o}}{\Delta T_1})^{NTU_g/NTU_o}$$

$$\frac{q_g}{q_o} = \frac{\Delta T_{r,g}}{\Delta T_1} \frac{\Delta T_1}{\Delta T_{r,o}}$$

Results of this comparison are shown in Figure 12. Assuming equal plate spacings, $D_{n,g} = D_{n,o}$, the Reynolds number ratio will be unity, $Re_{n,g} = Re_{n,o}$. Since surface 2 has a greater friction than surface 1, to achieve the same pumping power surface 2 must be shorter than surface 1, $L_g < L_o$. The magnitude of the NTU ratio is as shown. Since the NTU ratio and surface effectiveness are related as presented for case e, surface 2 will be more effective than surface 1. The heat transfer ratio will only be a function of the temperature rise ratio due to the constant flow rate between the two surfaces.

If surface 2 has a greater plate spacing than surface 1, $D_{n,g} > D_{n,o}$, then the Reynolds number of surface 2 is greater than surface 1, $Re_{n,g} > Re_{n,o}$. This will cause point g to move further to the right in Figure 8 and the above discussion is still applicable. If surface 2 plate spacing is less than surface 1, $D_{n,g} < D_{n,o}$, then the Reynolds number ratio will be less than unity, $Re_{n,g} < Re_{n,o}$, and point g may be located at g' in Figure 8. In this situation, surface 2 will have a greater length than surface 1, $L_g > L_o$, and the NTU ratio will increase and may exceed unity. This would cause a greater temperature ratio for surface 2 for any selected temperature ratio of surface 1, and subsequently an even greater heat transfer ratio.

An improved heat transfer for a shorter length heat exchanger at the same pumping power and frontal area is possible at some combination of surface parameters as indicated by Figure 12.
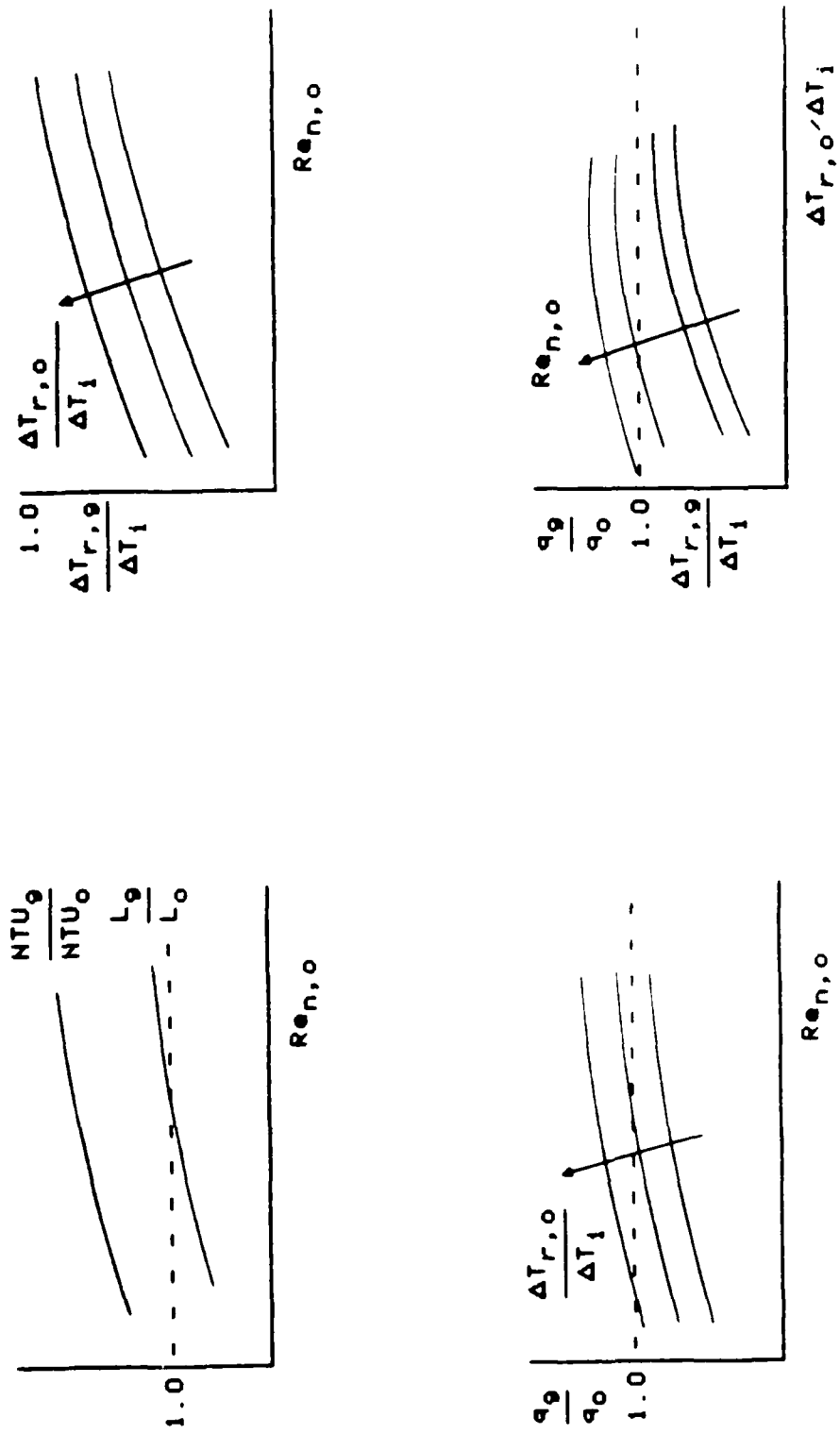
Figure 1.: Typical Performance Comparison Results for Case
q

IV. COMPARISON OF PLATE - FINNED SURFACES

The Kays and London plate - finned surfaces of reference
[3] that were considered are listed in Table II by surface
type, plate spacing, and surface designations. Only the
surfaces considered by Soland et al. [2] were analysed. Due
to the large number of surfaces considered, all the figures
on the following pages will use the numbering scheme listed
in the right hand column of Table II.

Soland showed that any surface performance curve which
is above the performance curve for another surface is a
better surface. A better surface is defined as one which
provides the same heat transfer rate for the same pumping
power, mass flow rate, and inlet temperatures - - case c.
The conclusion was that the wavy - fin plate - fin surface
17.8 - 3/8 W was the best surface for an aluminum heat
exchanger.

Refering to equations (8), (9), and (10) of Table I, if
two heat exchangers were constructed of the same surface but
different materials, then the surface with higher thermal
conductivity would result in a smaller heat exchanger. This
would primarily be due to a better fin efficiency and
subsequently a better overall surface efficiency. From
equation (16), a greater overall efficiency causes a larger
nominal Colburn j factor, $J_{n,2} > J_{n,1}$. Notice that the
nominal friction factor of equation (15) does not change.
These two items cause the performance curve for the higher

conductivity material to lie above the other and result in a smaller heat exchanger. If the two heat exchangers were constructed from different materials and different surfaces, fin efficiency may not improve due to higher thermal conductivity. In this situation, plate spacing, fin thickness, and conductivity play a role.

Performance curves for each surface listed in Table II were plotted for four different materials – – stainless steel, mild steel, aluminum, and copper. The surfaces were ranked by surface type for each material. To provide a more apparent comparison, aluminum was used as the base heat exchanger. Figures 13 through 16 are the performance curves obtained for stainless steel, mild steel, aluminum, and copper respectively. Only the best surface type constructed from aluminum is shown for each of the four materials.

TABLE II: KAYS AND LONDON PLATE - FIN SURFACES

| General Surface Type	Plate Spacing (b, inches)	Surface Designation	Surface Number
Plain Plate - Fin	.470	5.3	1
	.405	6.2	2
	.823	9.03	3
	.250	11.1	4
	.480	11.11(a)	5
	.330	14.77	6
	.418	15.08	7
	.250	19.86	8
Louvered Plate - Fin	.250	3.8-6.06	9
	.250	3/8(a)-6.06	10
	.250	1/2-6.06	11
	.250	1/2(a)-6.06	12
	.250	3/8-8.7	13
	.250	3/8(a)-8.7	14
	.250	3/16-11.1	15
	.250	1/4-11.1	16
	.250	1/4(b)-11.1	17
	.250	3/8-11.1	18
	.250	3/8(b)-11.1	19
	.250	1/2-11.1	20
	.250	3/4-11.1	21
	.250	3/4(b)-11.1	22
Strip - Fin Plate - Fin	.250	1/4(b)-11.1	23
	.485	3/32-12.22	24
	.414	1/8-15.2	25
Wavy - Fin Plate - Fin	.413	11.44-3/8 W	26
	.413	17.8-3/8 W	27
Pin - Fin Plate - Fin	.240	AP-1	28
	.398	AP-2	29
	.750	PF-3	30
	.502	PF-4(F)	31
	.510	PF-9(F)	32

Figure 13: Performance Parameter Curves of Plate - Finned Surfaces for Stainless Steel.
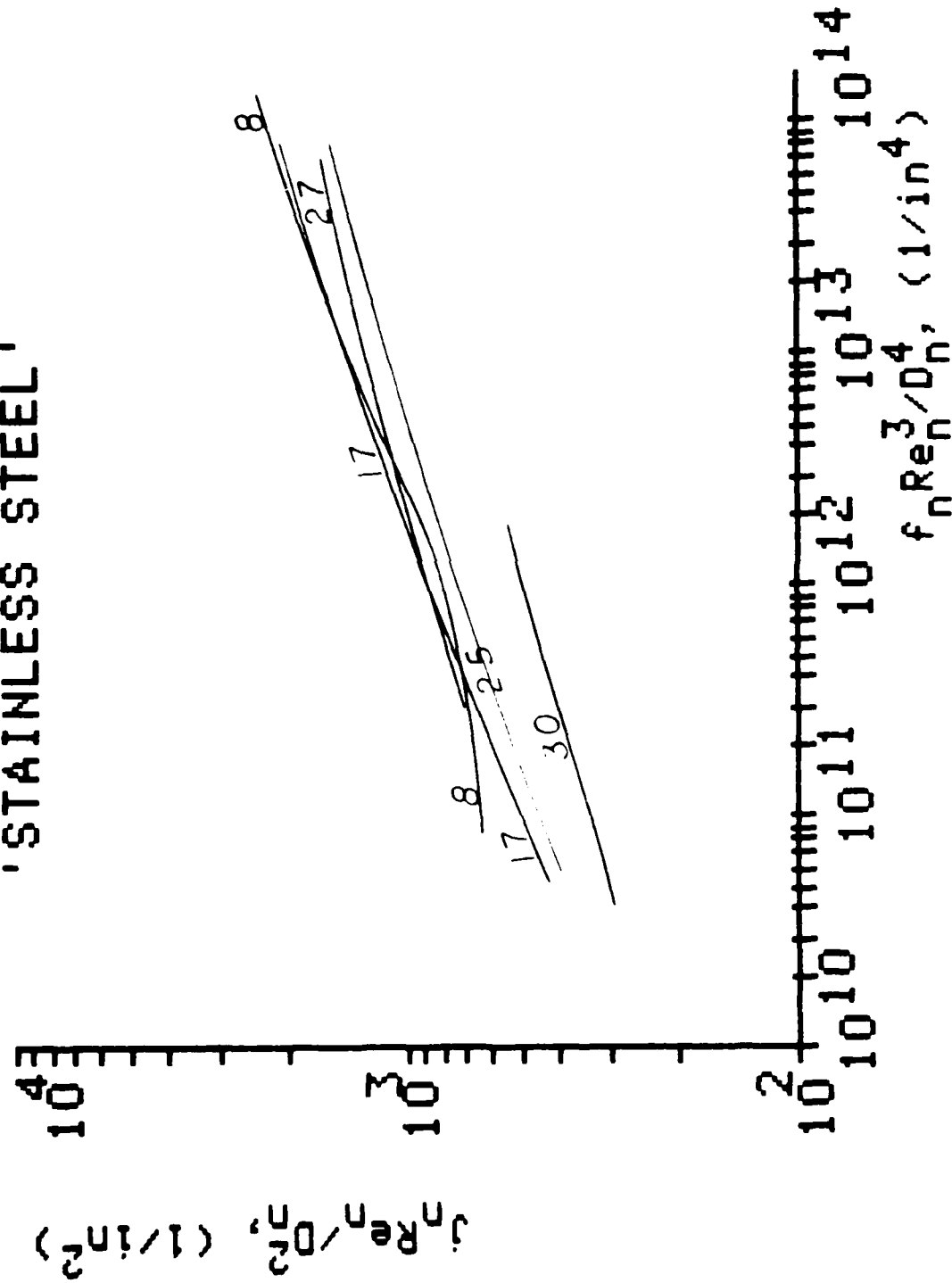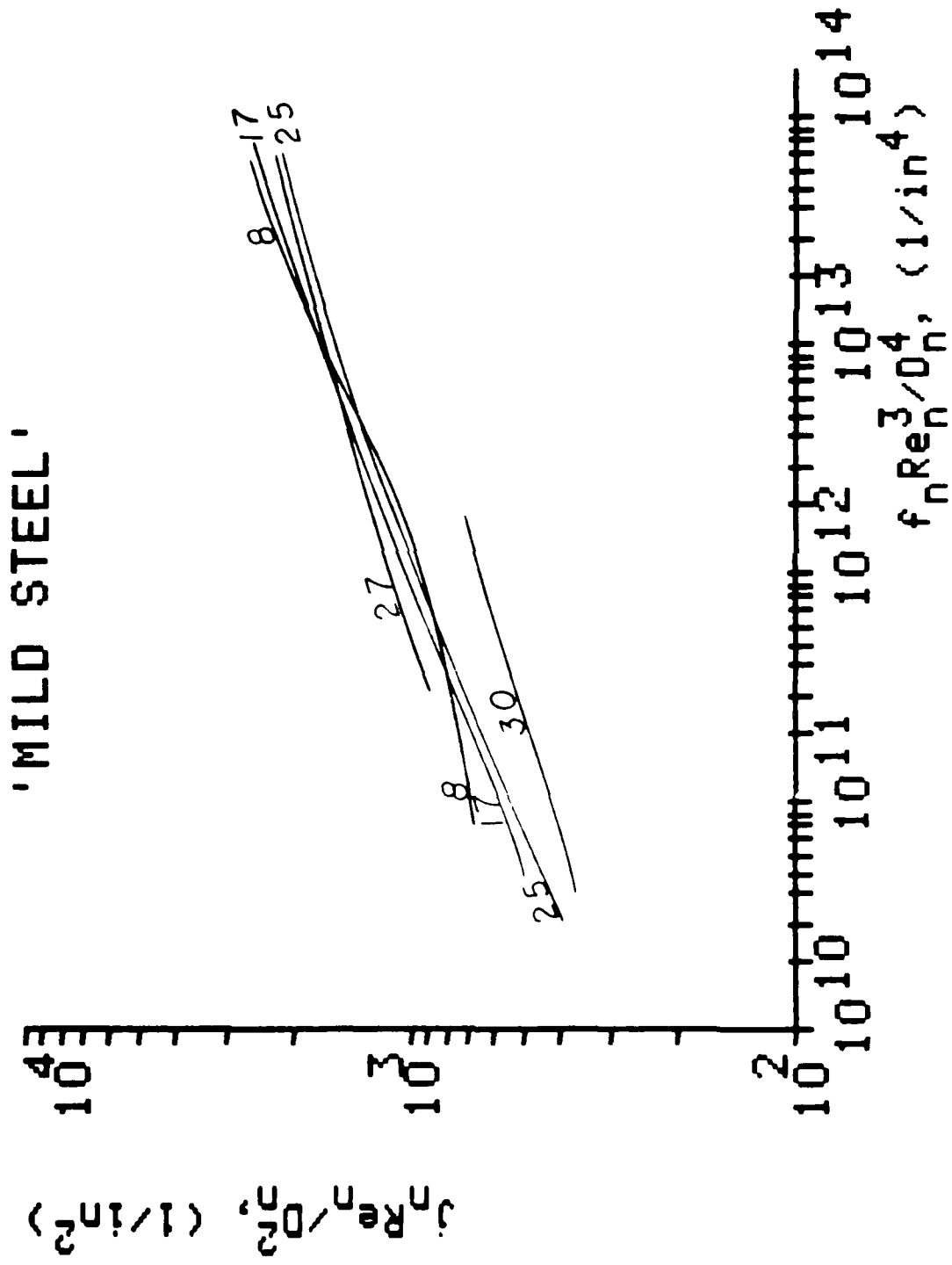
Figure 14: Performance Parameter Curves of Plate – Finned Surfaces for Mild Steel.
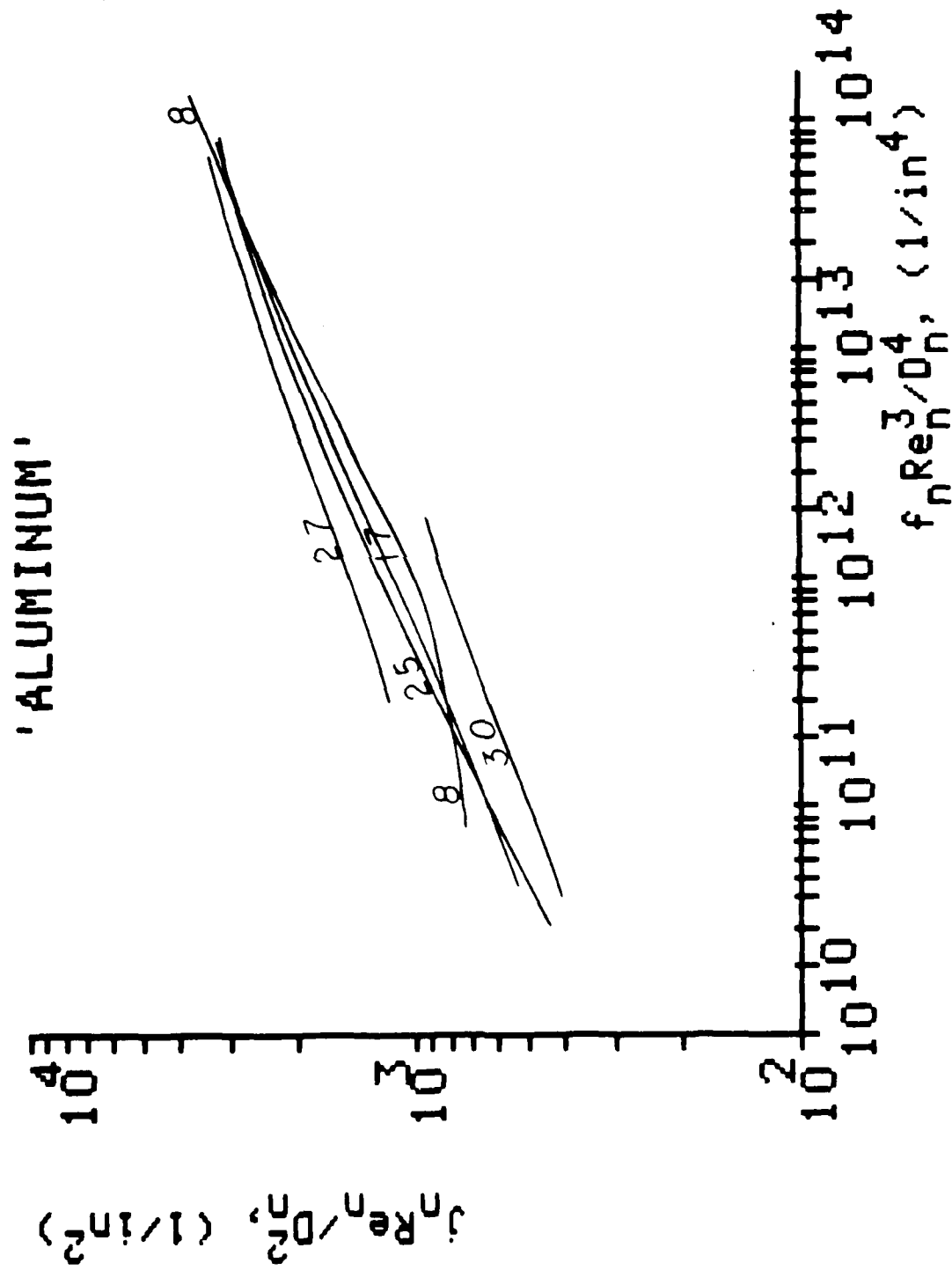
'ALUMINUM'

Figure 15: Performance Parameter Curves of Plate - Finned
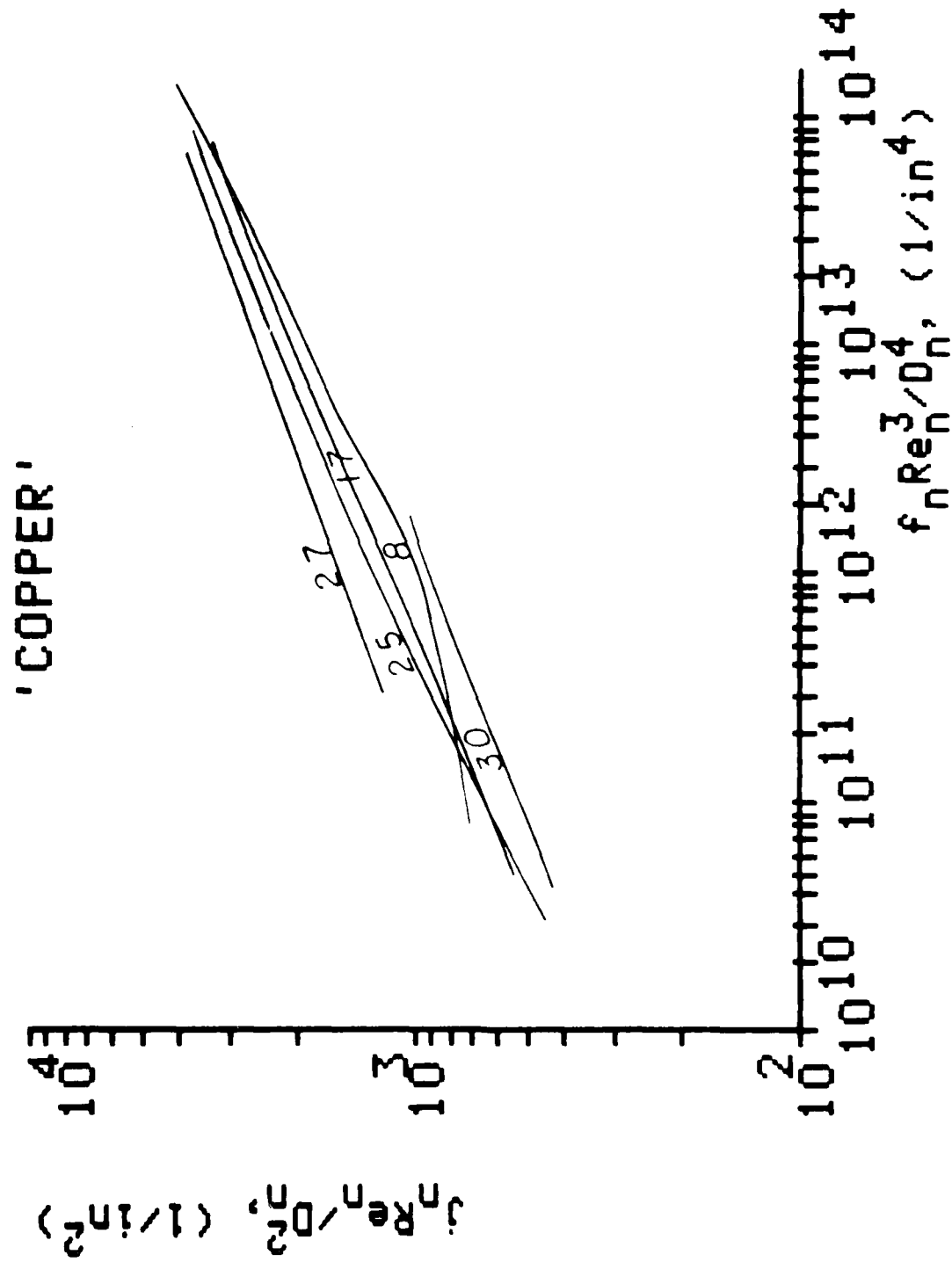Surfaces for Aluminum.

Figure 10: Performance Parameter Curves of Plate - Finned
Surfaces for Copper.

To perform a comparison of cases e, f, and g, a reference surface was selected. This surface is a smooth surface with no enhancements and a plate spacing of 0.25 inches (D_n = 0.5 inches). Comparison of many surfaces to a single common smooth plate nominal hydraulic diameter permits a relative comparison between surfaces having different nominal diameters.

The performance curve ordinate, J_n/D_n, for a smooth surface was determined utilizing the turbulent flow in tubes Colburn correlation for forced convection from reference [4]:

$$j = 0.023 \, Re^{-0.2} \qquad (26)$$

For a smooth surface $h = h_n$, $G = G_n$, $Re = Re_n$. Then:

$$\frac{j_s}{D_n} = \frac{0.023 \, Re^{-0.2}}{D_n} \qquad (27)$$

The performance curve abscissa, $f_n Re_n^2/D_n^3$, for a smooth surface was calculated by the linear approximation from reference [4]:

$$f = 0.0791 \, Re^{-0.25} \qquad (28)$$

For a smooth surface $f = f_n$.

$$\frac{f_s Re_n^2}{D_n^3} = \frac{0.0791 \, Re_n^{1.75}}{D_n^3} \qquad (29)$$

Solving equation (28) for Re_n and substituting into equation (27) leads to:

$$\frac{j_s}{D_n} = \frac{0.0172}{D_n^{1.343}} \, (f_s Re_n^2/D_n^3)^{-0.114} \qquad (30)$$

Equation (30) provides the performance curve for a smooth surface for cases e, f, and g. Figure 17 shows the performance curves used for these comparisons. Shown are the best surface of each surface type determined by case c and the smooth surface for aluminum heat exchanger material. In the following figures, the subscript "es" will denote the enhanced surface and the subscript "s" will denote the smooth surface.

Results for case e, same shape, volume, and pressure drop, are shown in Figures 18 through 23 inclusive. Figure 18 shows the NTU ratio as a function of $Re_{n,s}$. The flow rate ratio, which is equivalent to the pumping power ratio, is shown in Figure 19. Note that in Figure 19, a higher ratio is the smaller pumping power for the enhanced surface. Since a family of curves are generated for the heat transfer and temperature rise ratios, Figures 20 and 21, only the curves for a smooth surface temperature rise ratio of 0.1 are shown. A family of curves generated by the selected smooth surface temperature rise ratio are shown in Figures 22 and 23 for heat transfer and temperature rise ratios. These figures show the results for one surface only, namely the plain plate - finned surface 6.2. Ratios of heat transfer and temperature rise as a function of the smooth surface temperature rise are shown in Figures 24 and 25 respectively for the same surface.

For case f, same frontal area, flow rate, and heat transfer, Figures 26 and 27 show the results. Figure 26 is the pumping power ratio and Figure 27 is the length ratio as a function of the smooth surface nominal Reynolds number, $Re_{n,s}$. A lower ratio is preferred in Figure 26, and a higher ratio in Figure 27.

Case g results are shown in Figures 28 through 35 inclusive. The NTU ratio is shown in Figure 28 and the length ratio in Figure 29. Like case e, heat transfer ratio vs. $Re_{n,s}$ is Figure 30 and temperature rise ratio vs. $Re_{n,s}$ is Figure 31 for an inlet temperature rise ratio of 0.1 on the smooth surface. A family of curves generated by the selected smooth surface temperature rise ratio are shown in Figures 32 and 33 for heat transfer and temperature rise ratios. These figures show the results for one surface only, namely the plain plate - finned surface 6.2. Figures 34 and 35 show a family of curves for the heat transfer and temperature rise ratios respectively, vs. the smooth surface temperature rise ratio for the same single surface. In Figure 29 a higher ratio gives better results and in Figures 28, 30, and 31 a lower ratio is preferable.
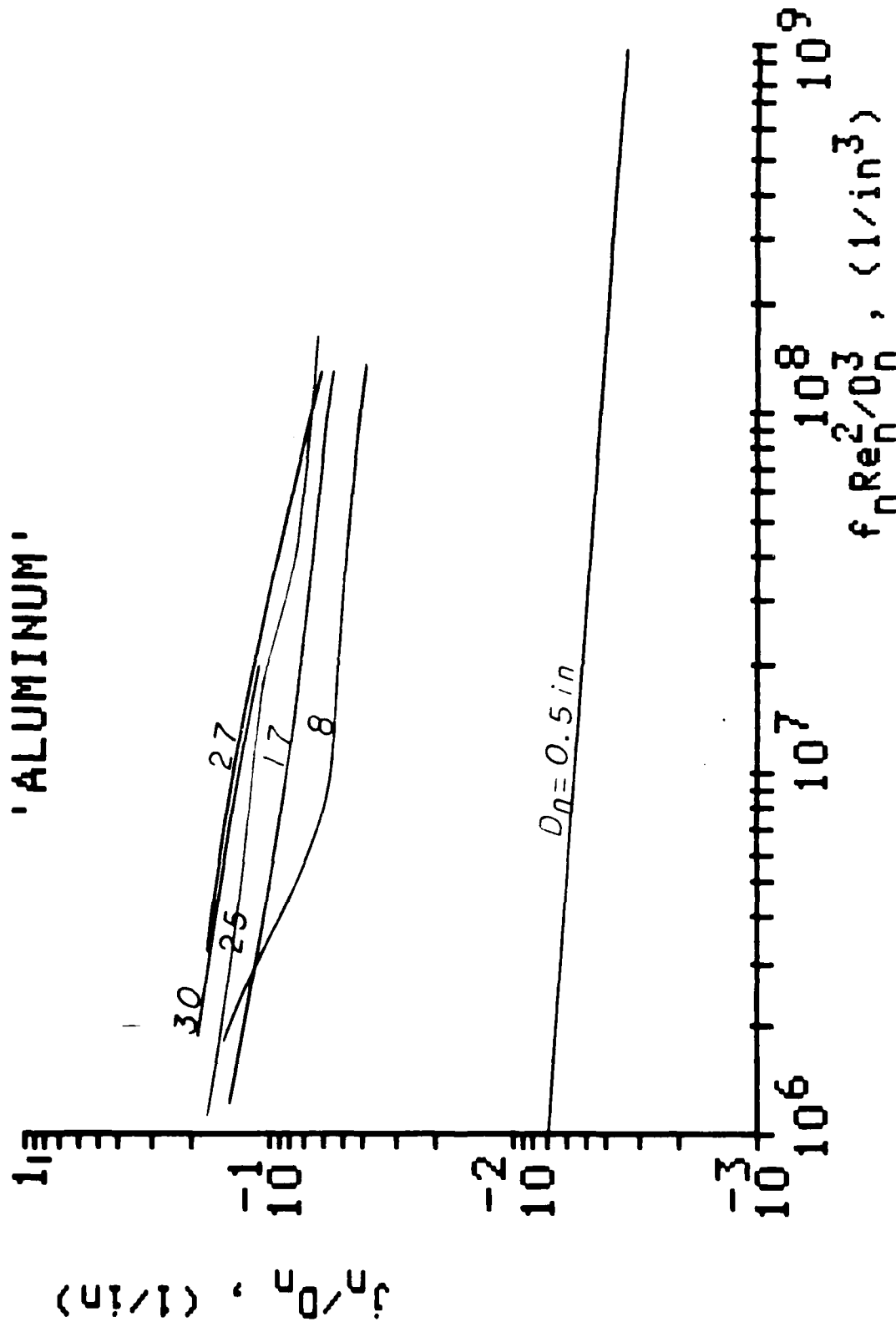
'ALUMINUM'

$D_n = 0.5 in$

j_n/O_n, (1/in)

$f_n Re_n^2/O_n^3$, (1/in^3)

Figure 1. Performance Parameter Curves of Plate - Finned
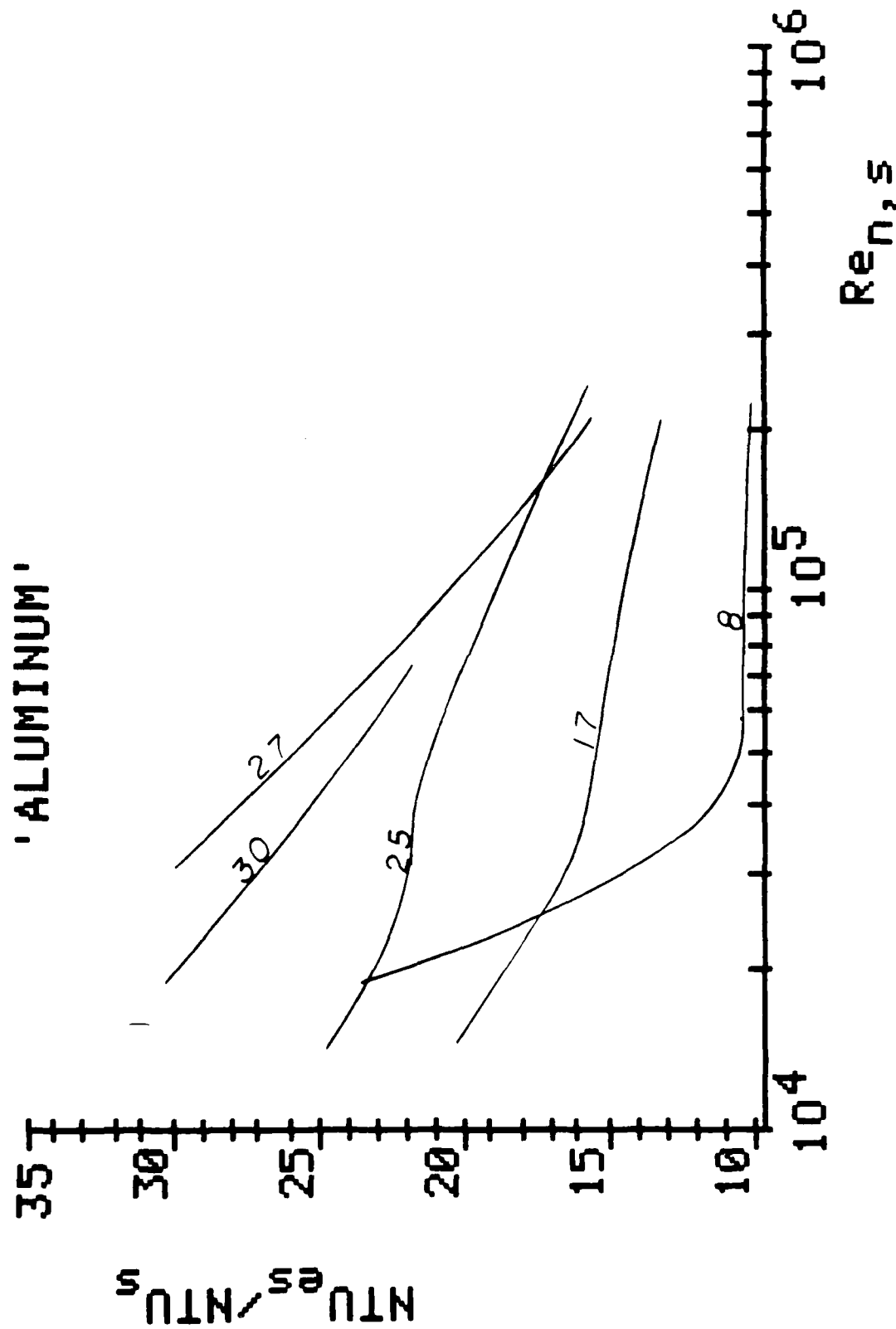surfaces for cases e, f, and g.

Figure 18: Performance Comparison Results of Number of Heat
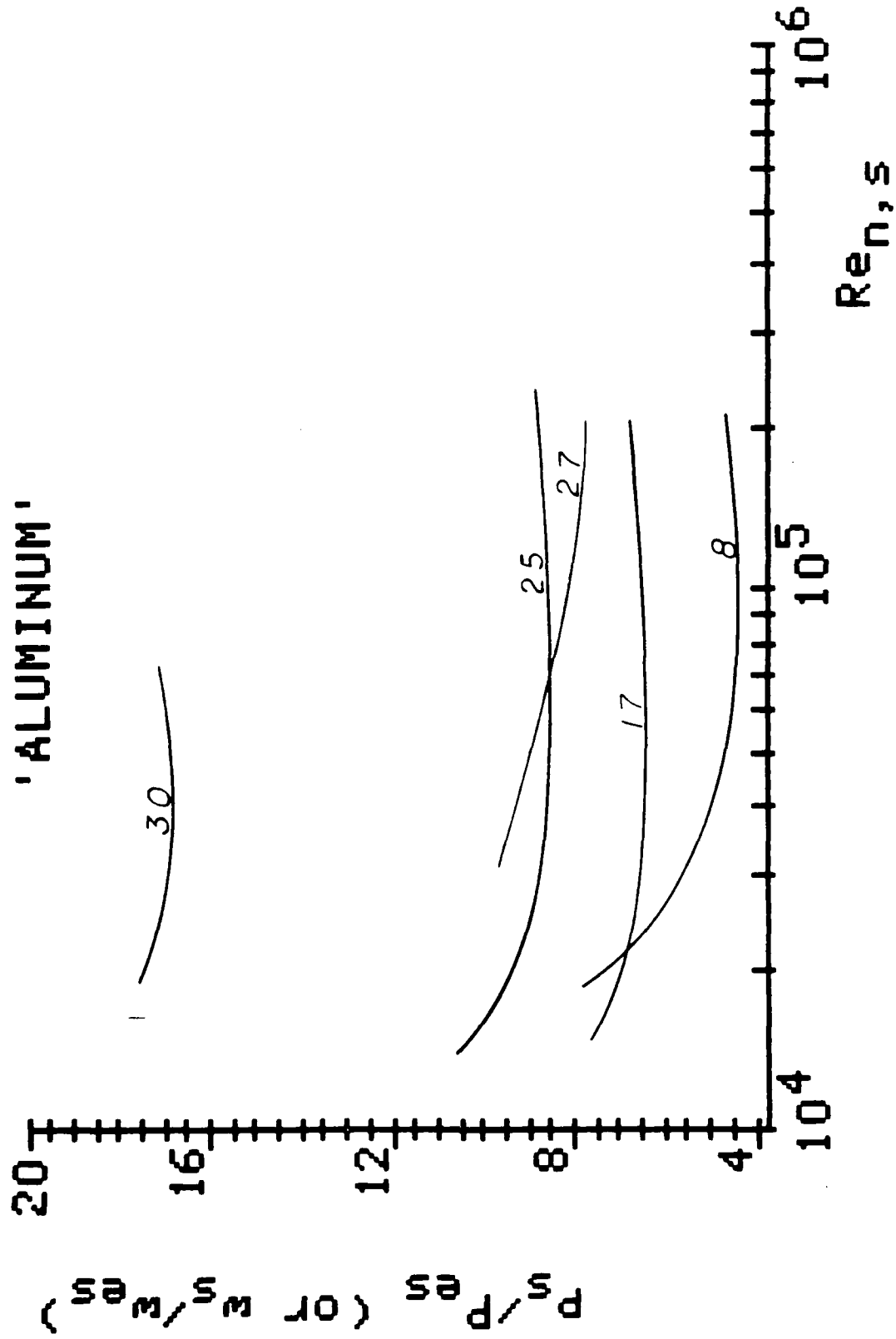Transfer Units for Case e.

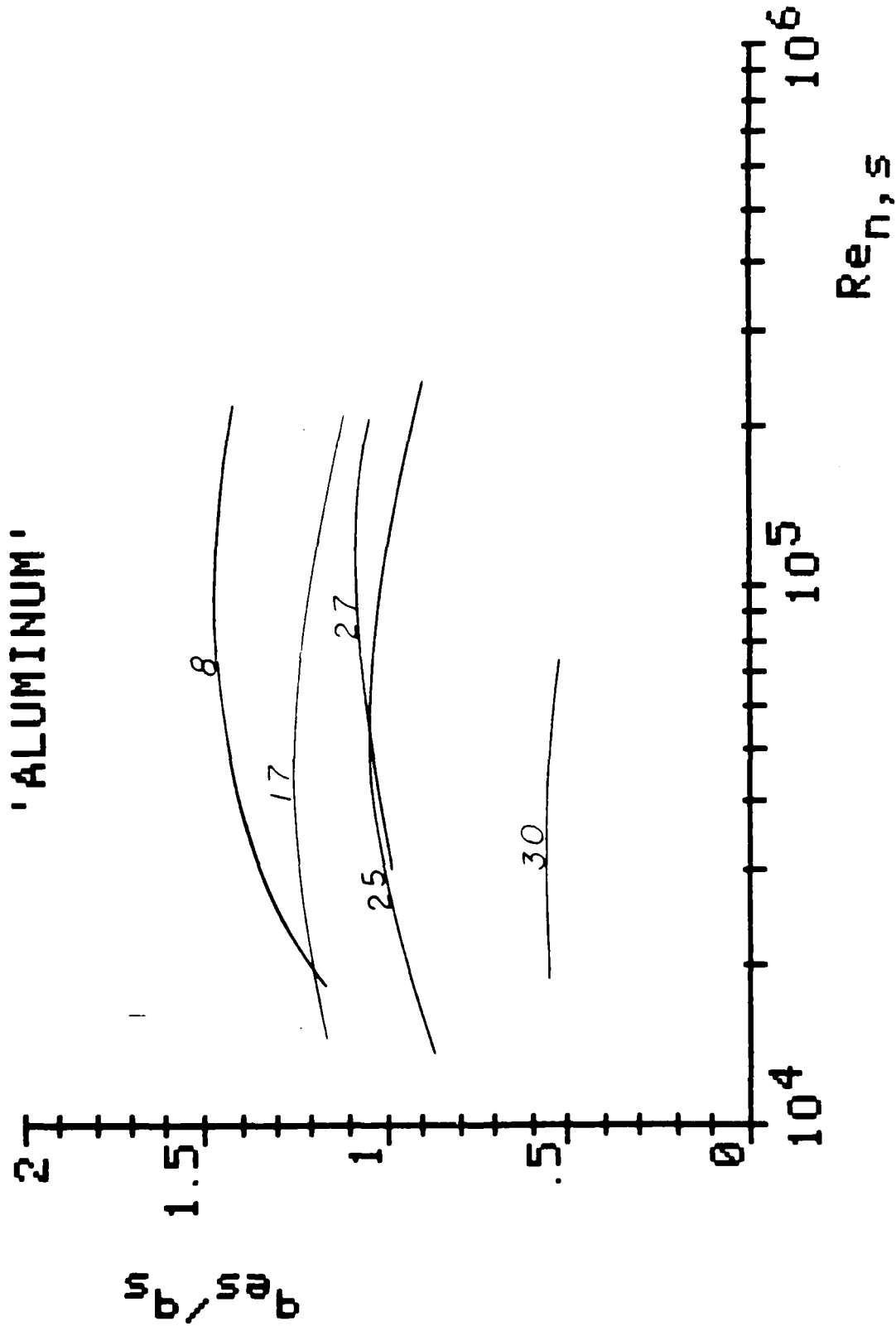Figure 19: Performance Comparison Results of Pumping Power for Case e.

Figure 20: Performance Comparison Results of Heat Transfer for Case e and $\Delta T_{r,s}/\Delta T_i = 0.1$.
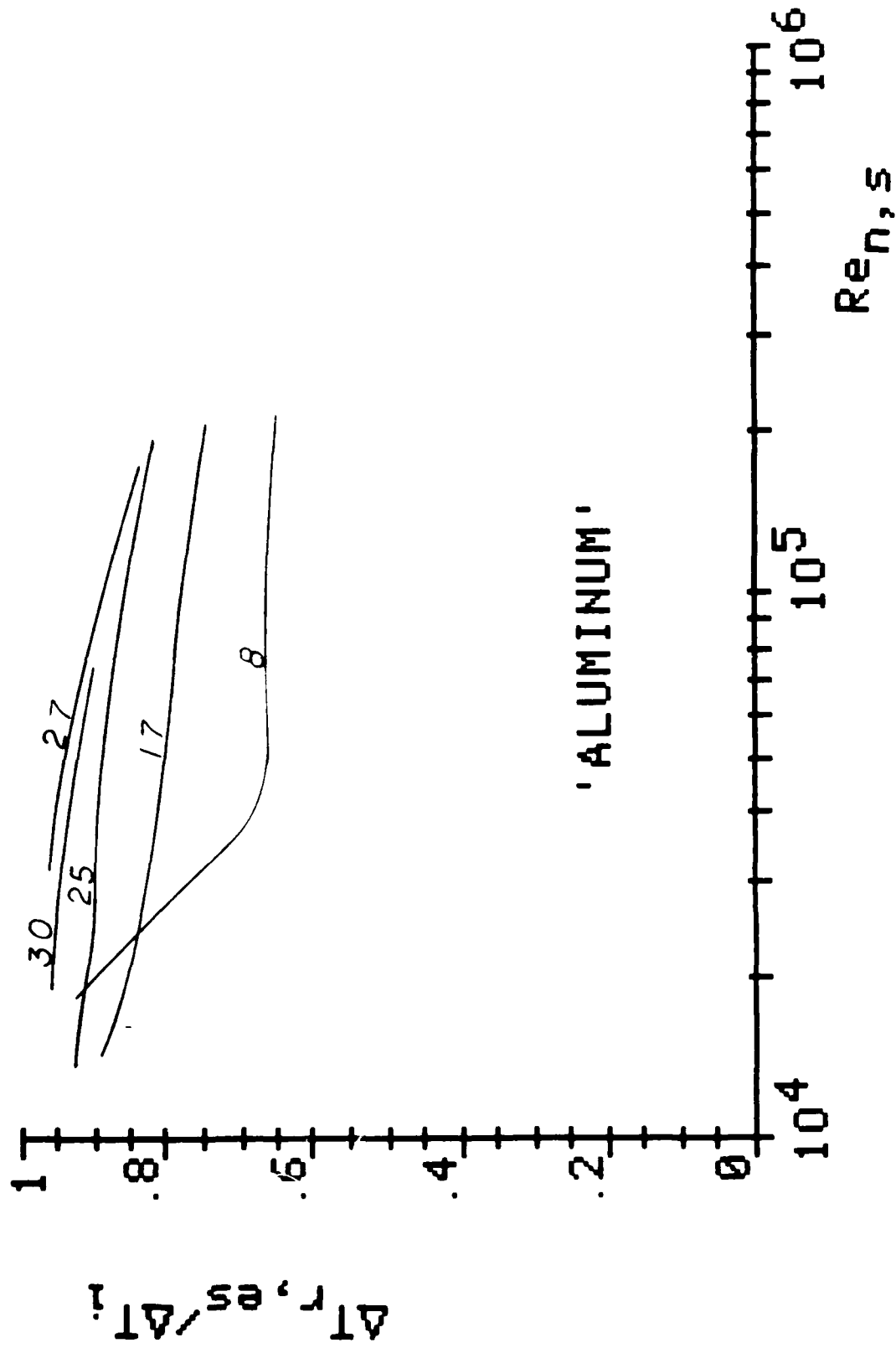
Figure 21: Performance Comparison Results of Temperature Rise for Case e and $\Delta T_{r,s}/\Delta T_i = 0.1$.
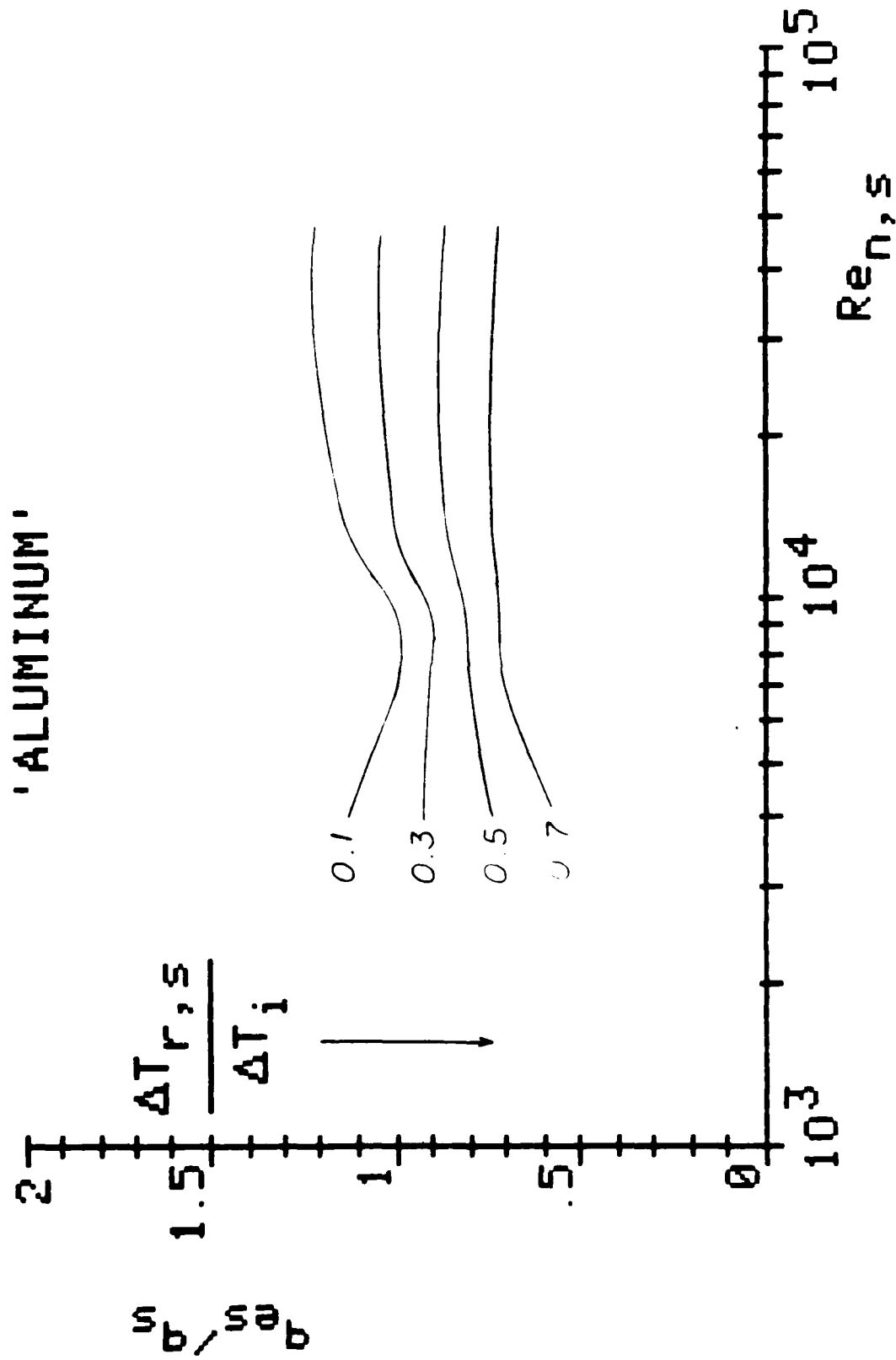
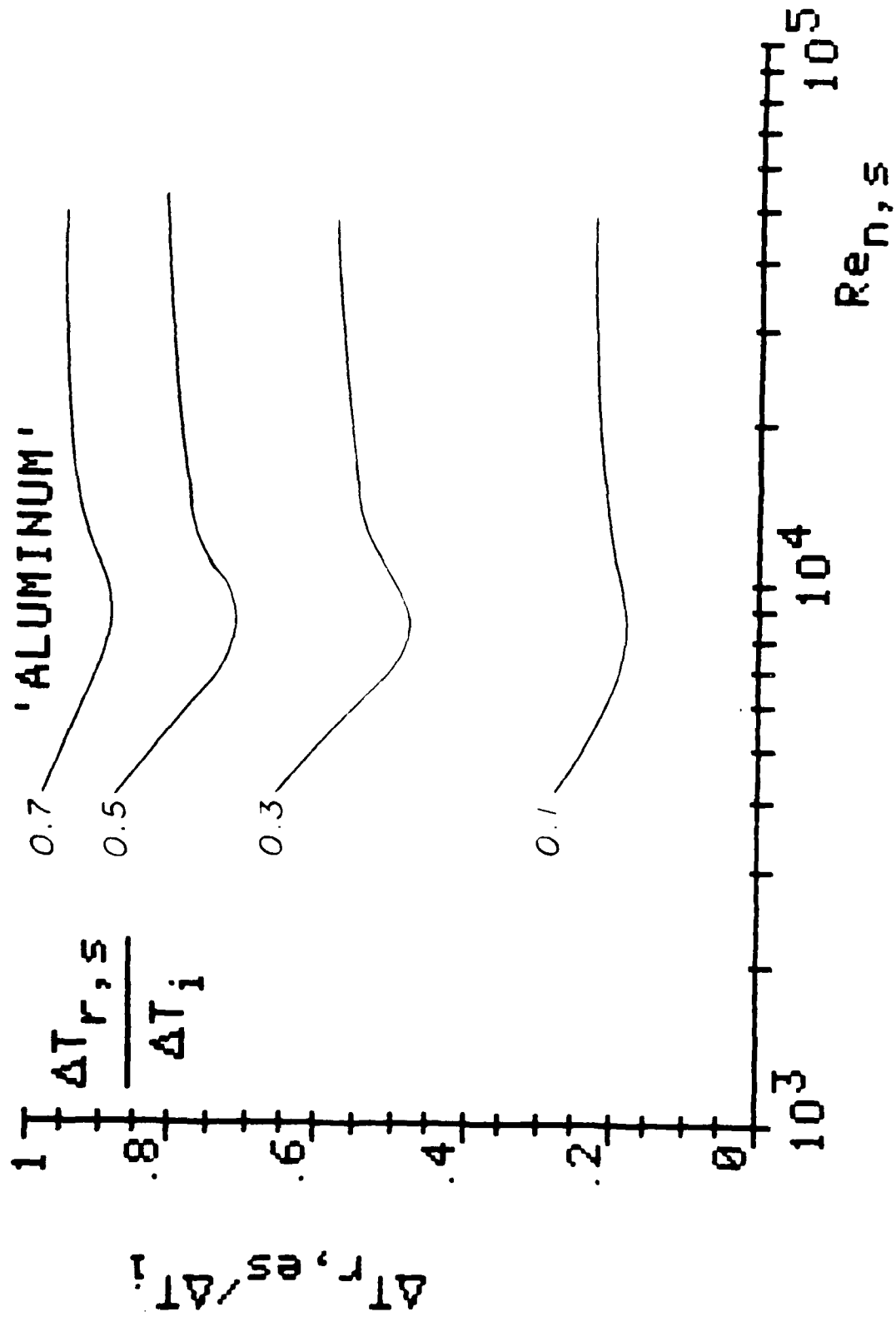Figure 2.2: Performance Comparison Results of Heat Transfer for Plain Plate - Finned Surface 6.2 for Case e.

Figure 2.3: Performance Comparison Results of Temperature Rise for Plain Plate - Finned Surface 6.2 for Case e.
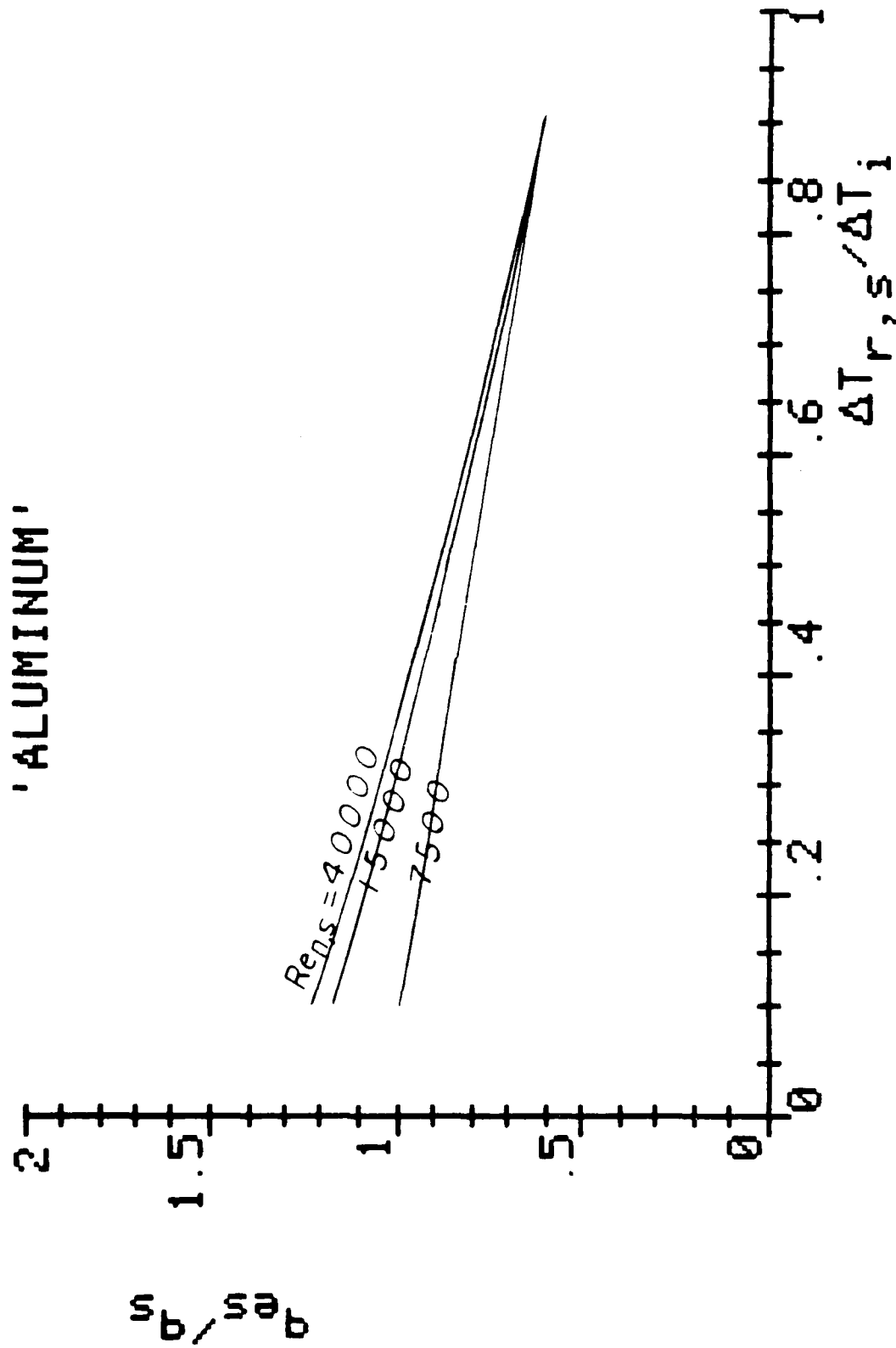
Figure 24: Heat Transfer for Plain Plate - Finned Surface
h. ℓ vs. Smooth Surface Temperature Rise for Case
ℓ

Figure .5: Temperature Rise for Plain Plate - Finned
Surface t.2 vs. Smooth Surface Temperature Rise
for Case e.

Figure 26: Performance Comparison Results of Pumping Power for Case t.

Figure ... Performance Comparison Results of Length for Case t.
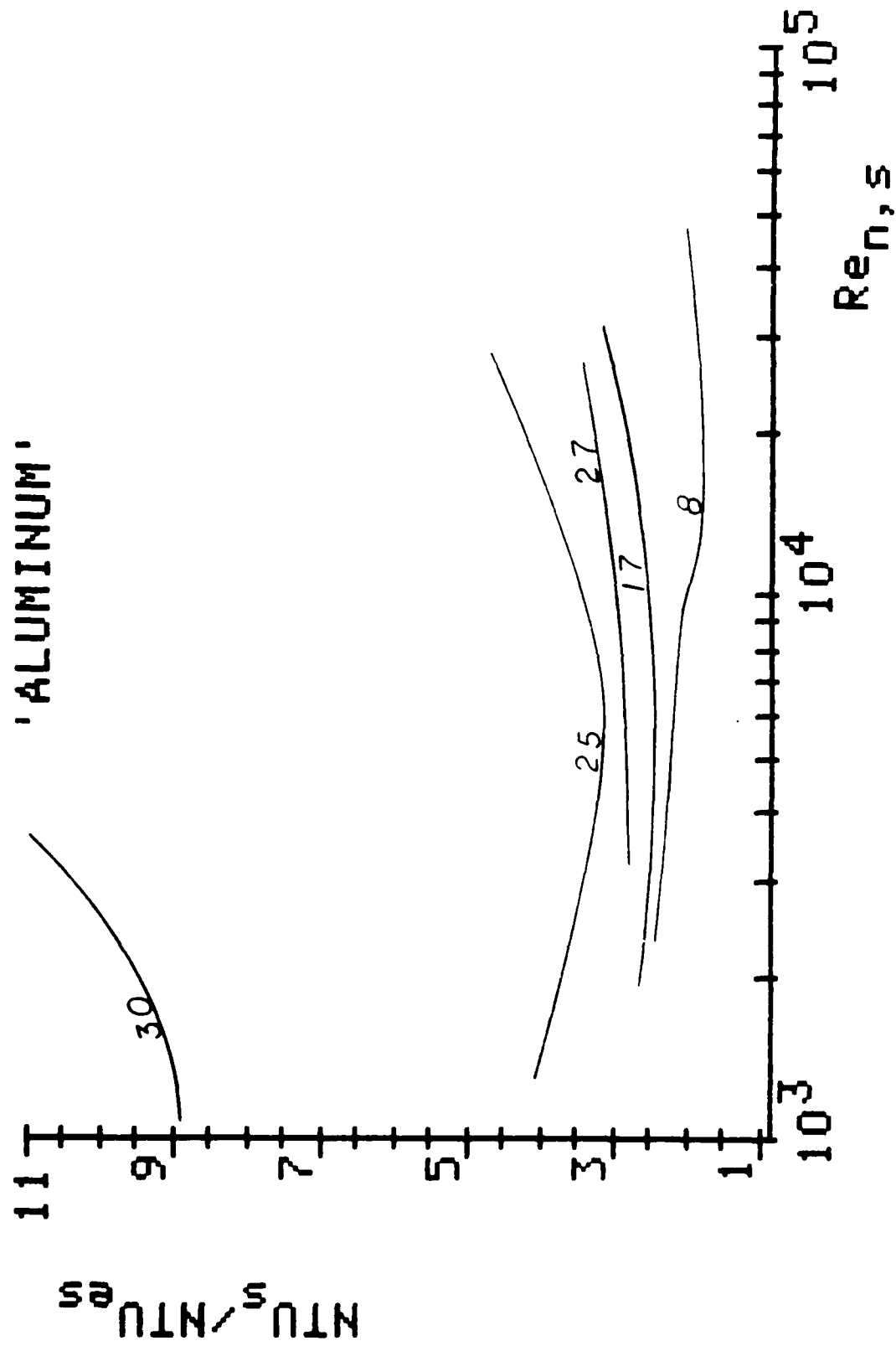
Figure 28: Performance Comparison Results of Number of Heat Transfer Units for Case 9.
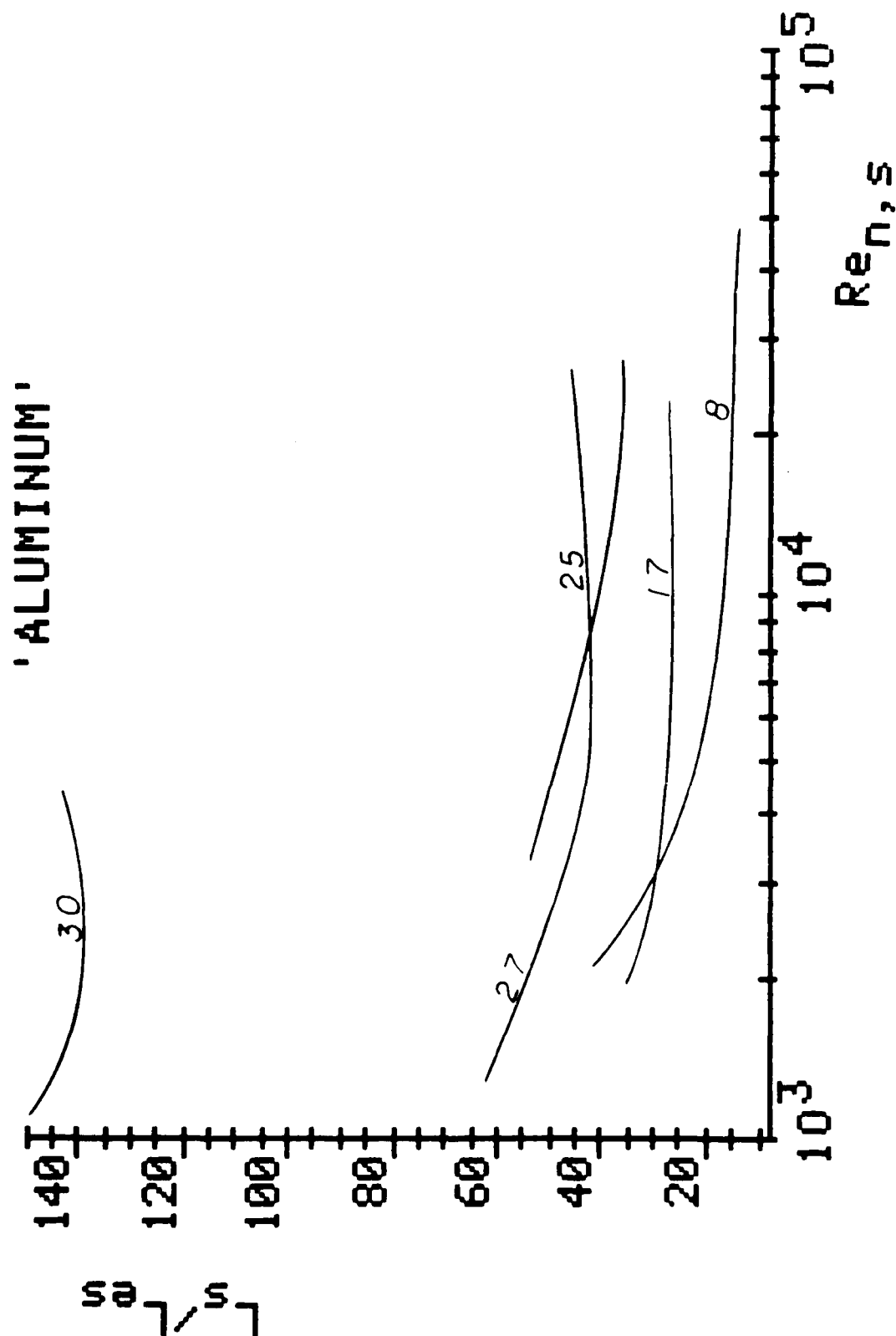
Figure 20: Performance Comparison Results of Length for Case 9.
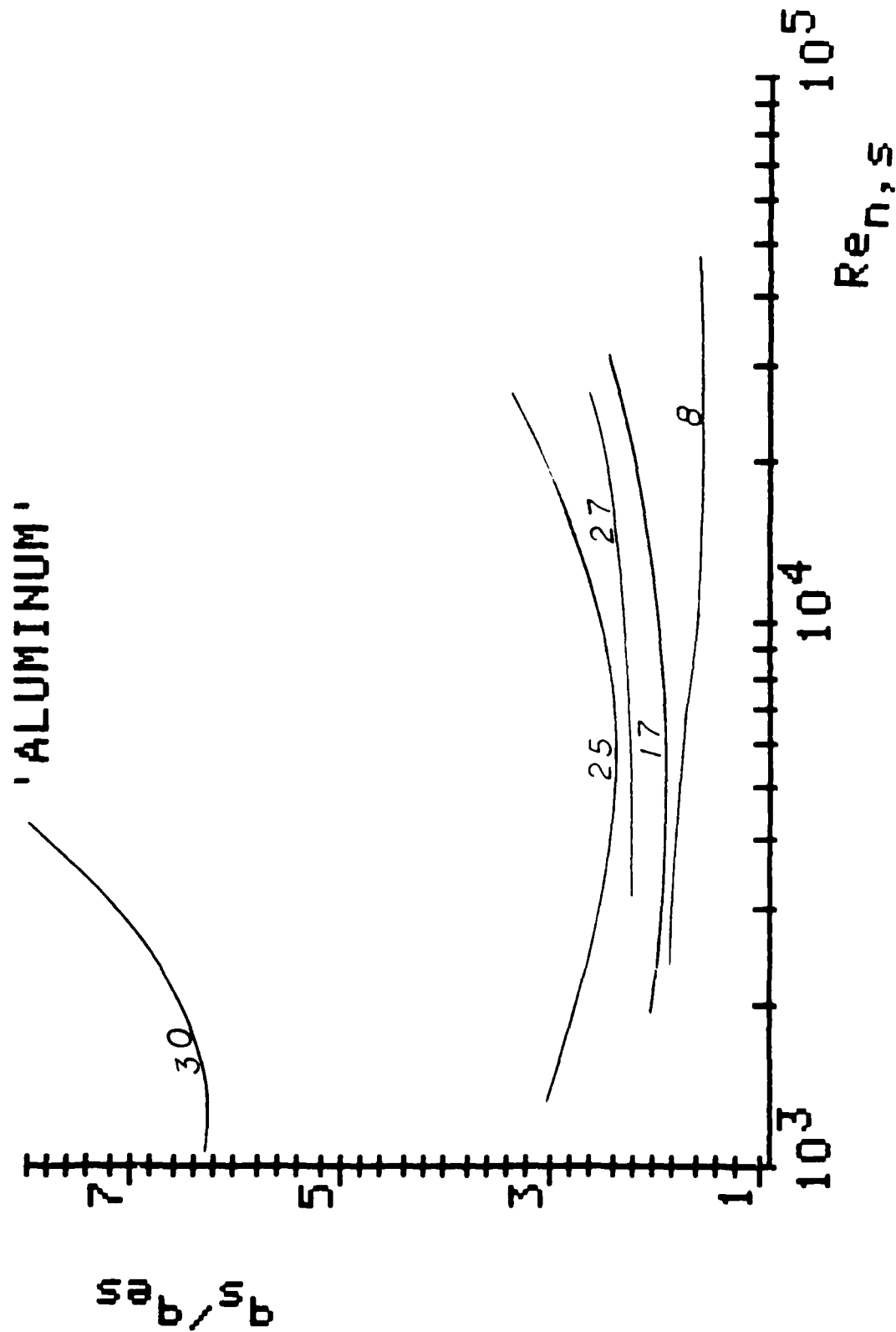
Figure 30: Performance Comparison Results of Heat Transfer for Case g and $\Delta T_{r,s}/\Delta T_i = 0.1$.
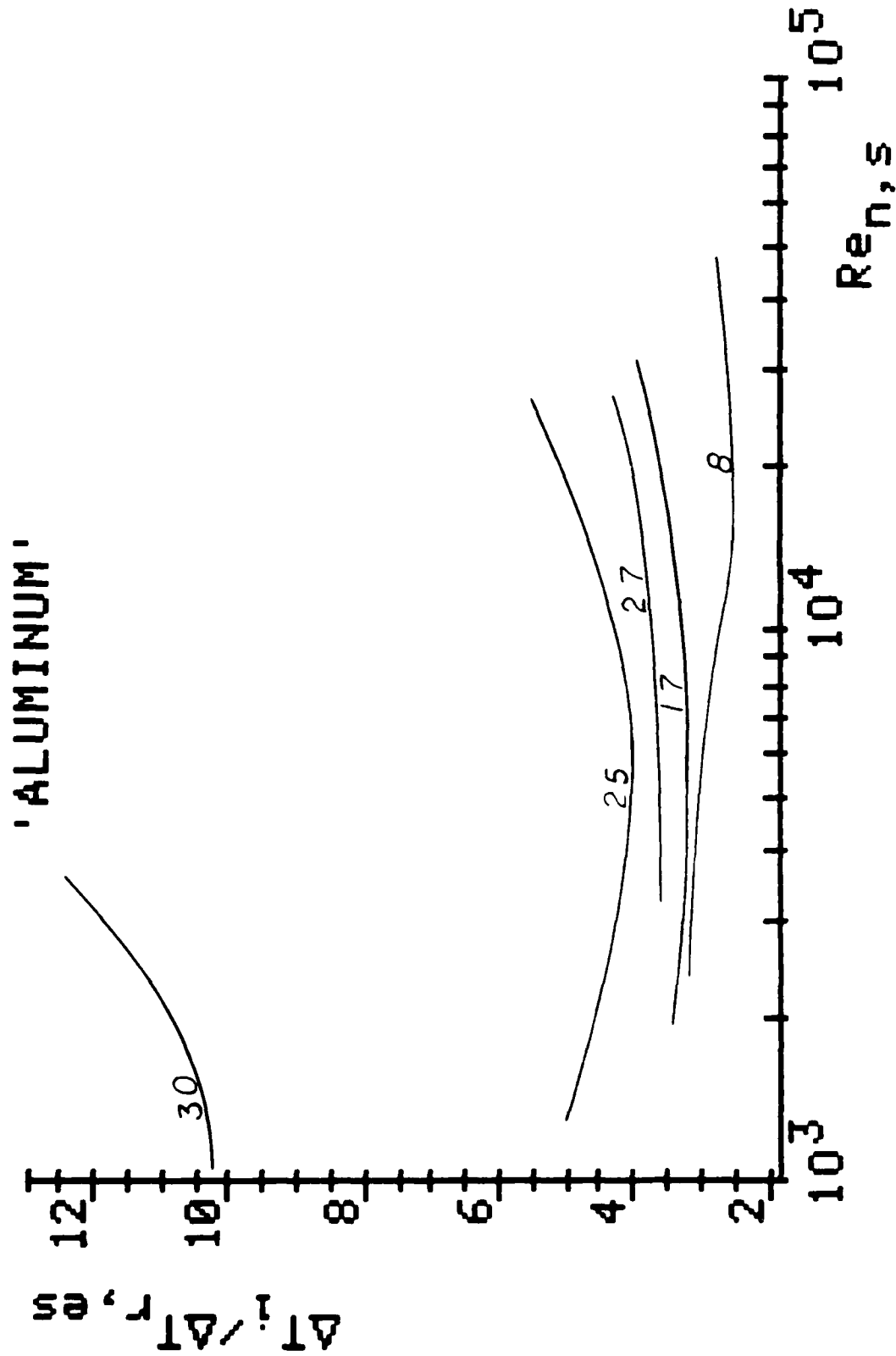
Figure 31: Performance Comparison Results of Temperature
Rise for Case g and $\Delta T_{r,s}/\Delta T_i = 0.1$.
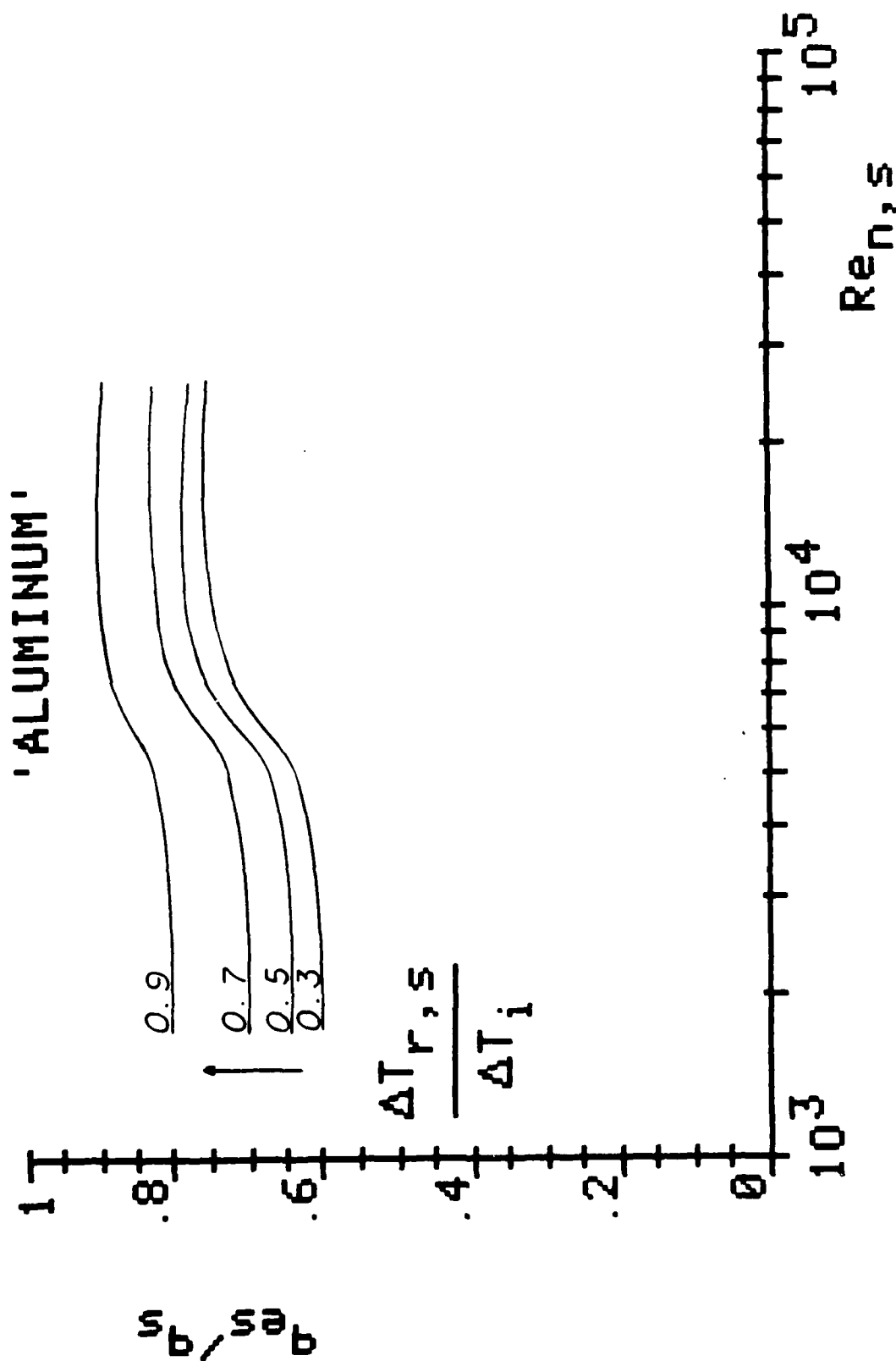
Figure 31: Performance Comparison Results of Heat Transfer for Plain Plate - Finned Surface 6.2 for Case 9.
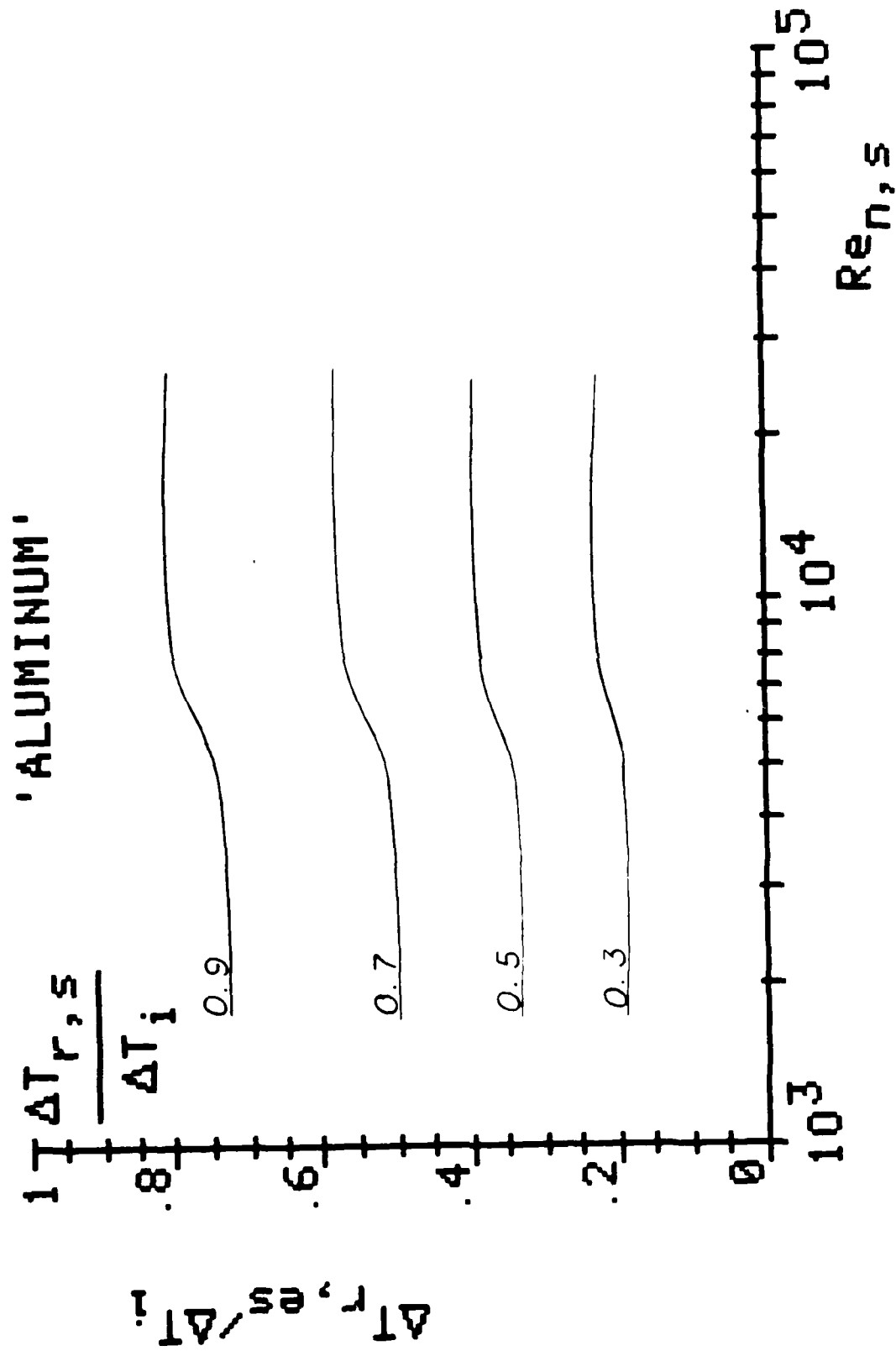
Figure 31: Performance Comparison Results of Temperature Rise for Plain Plate - Finned Surface 6.2 for Case 9.
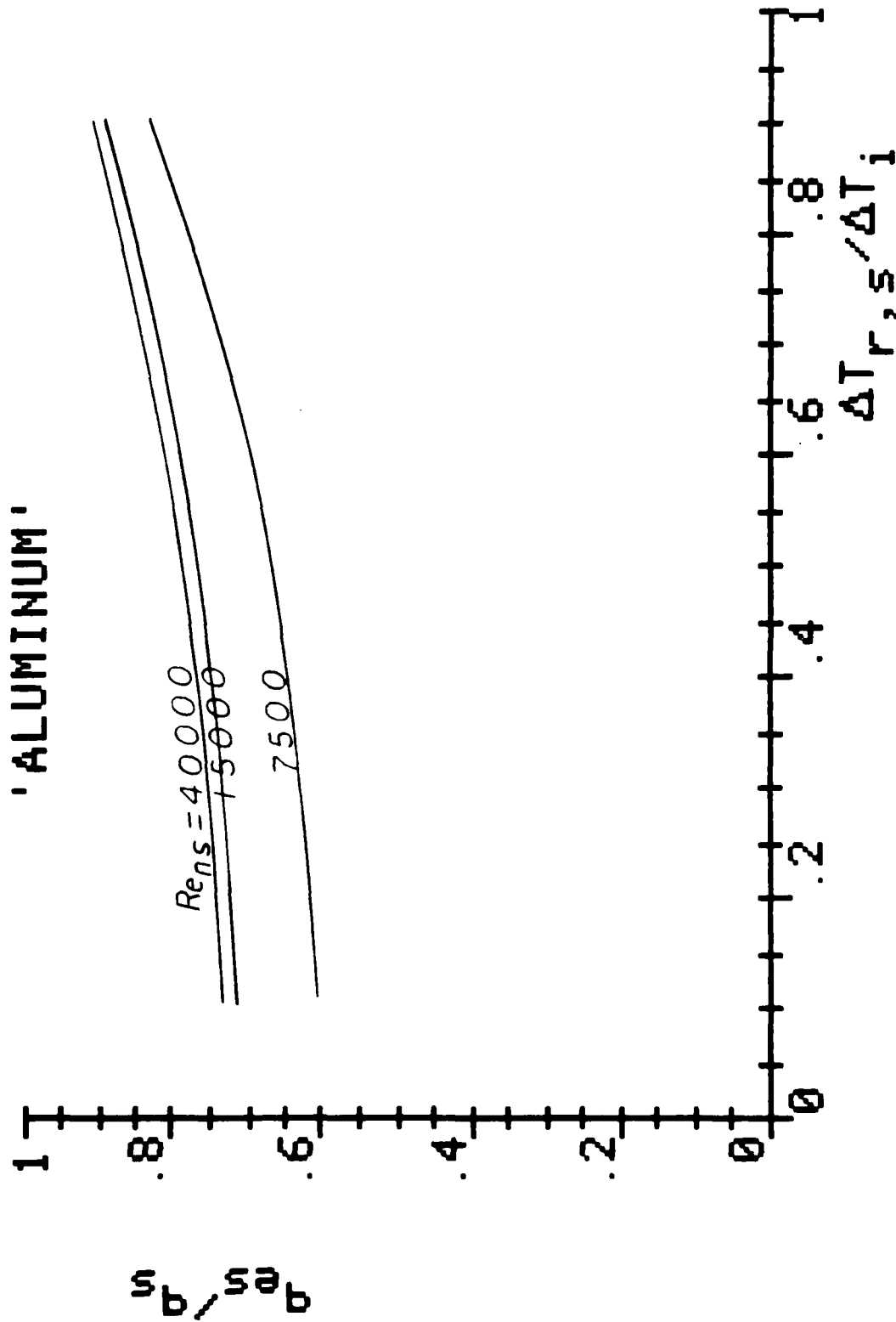
Figure 34: Heat Transfer for Plain Plate - Finned Surface $q_{r,s}$ vs. Smooth Surface Temperature Rise for Case 9.
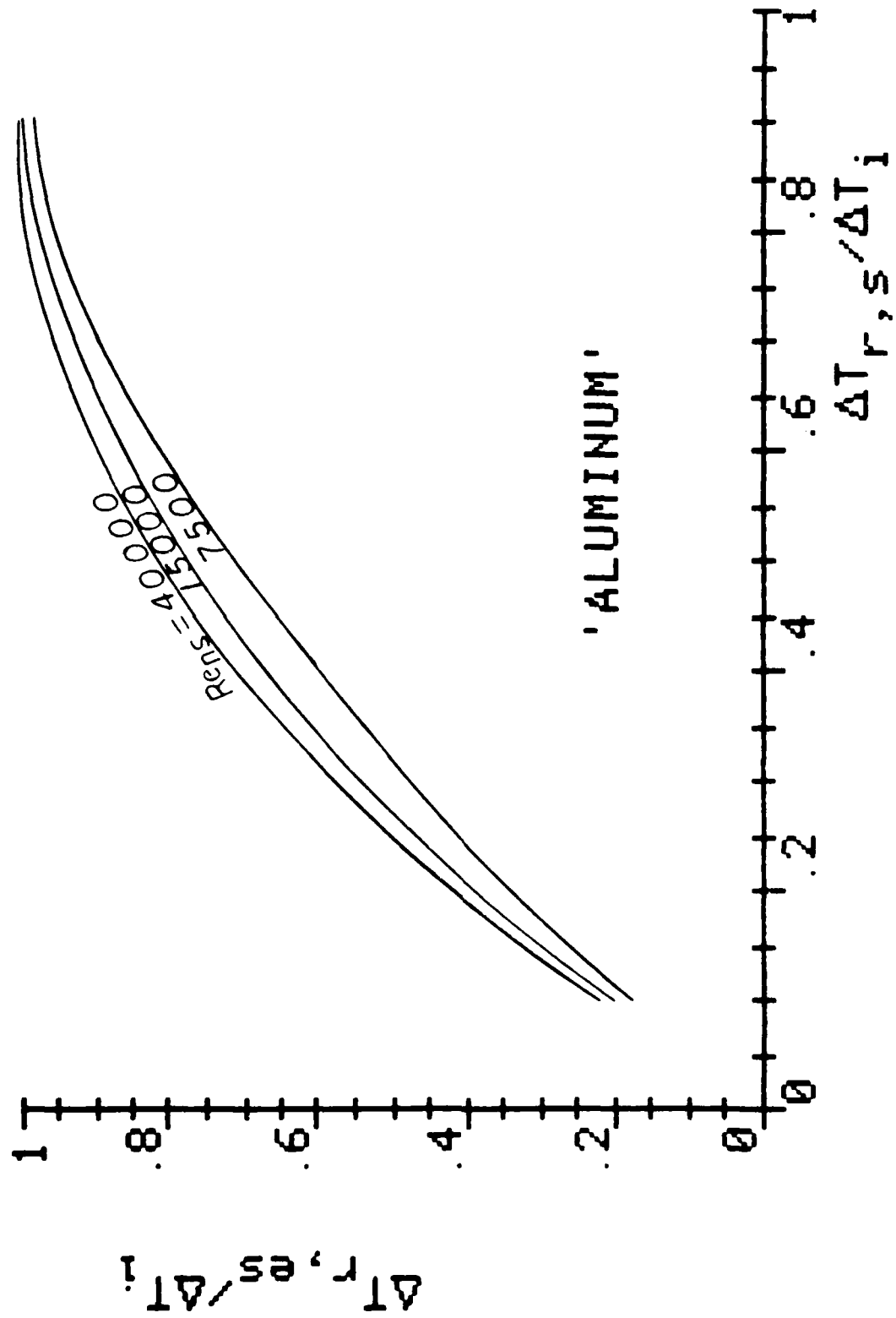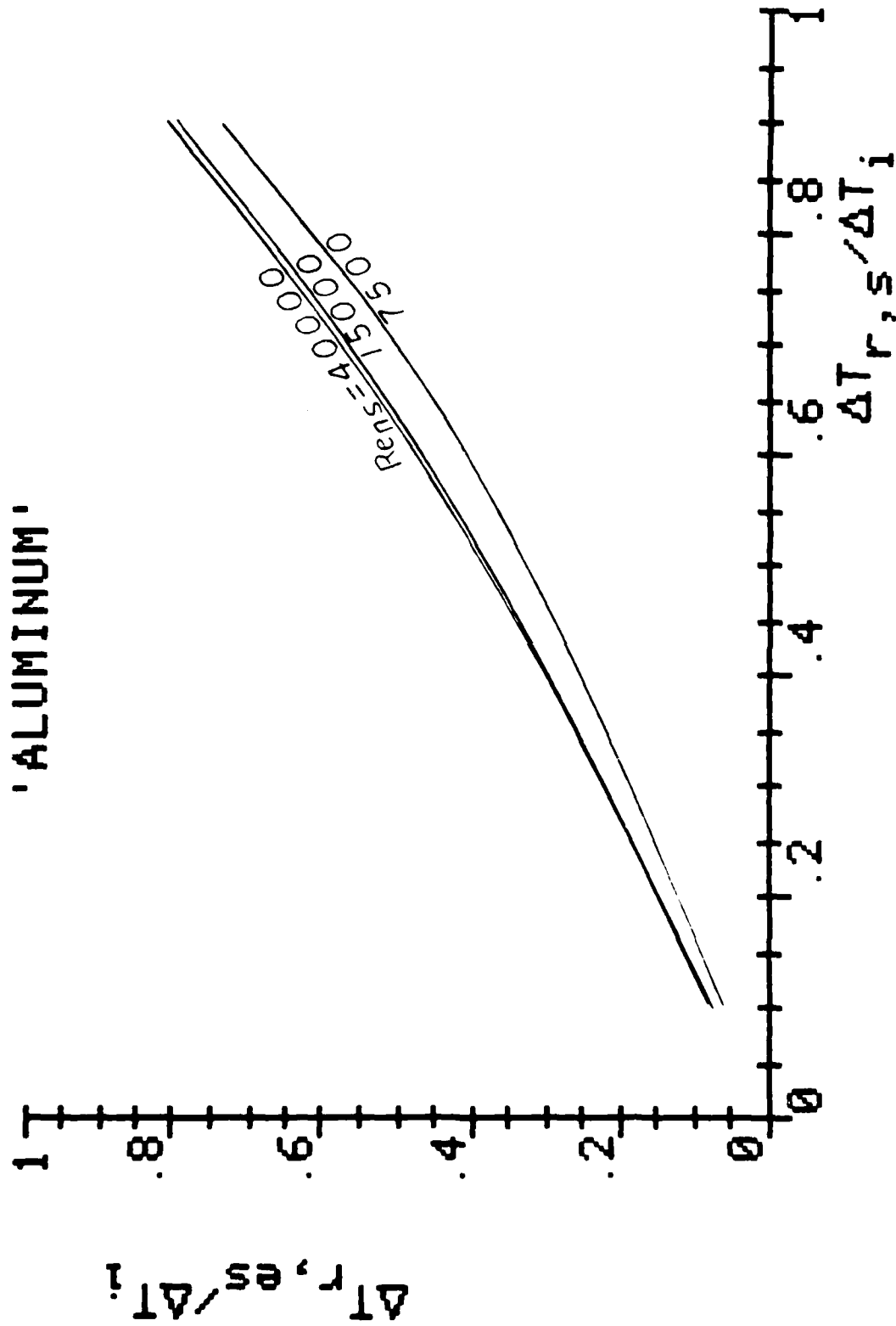
Figure 35: Temperature Rise for Plain Plate - Finned
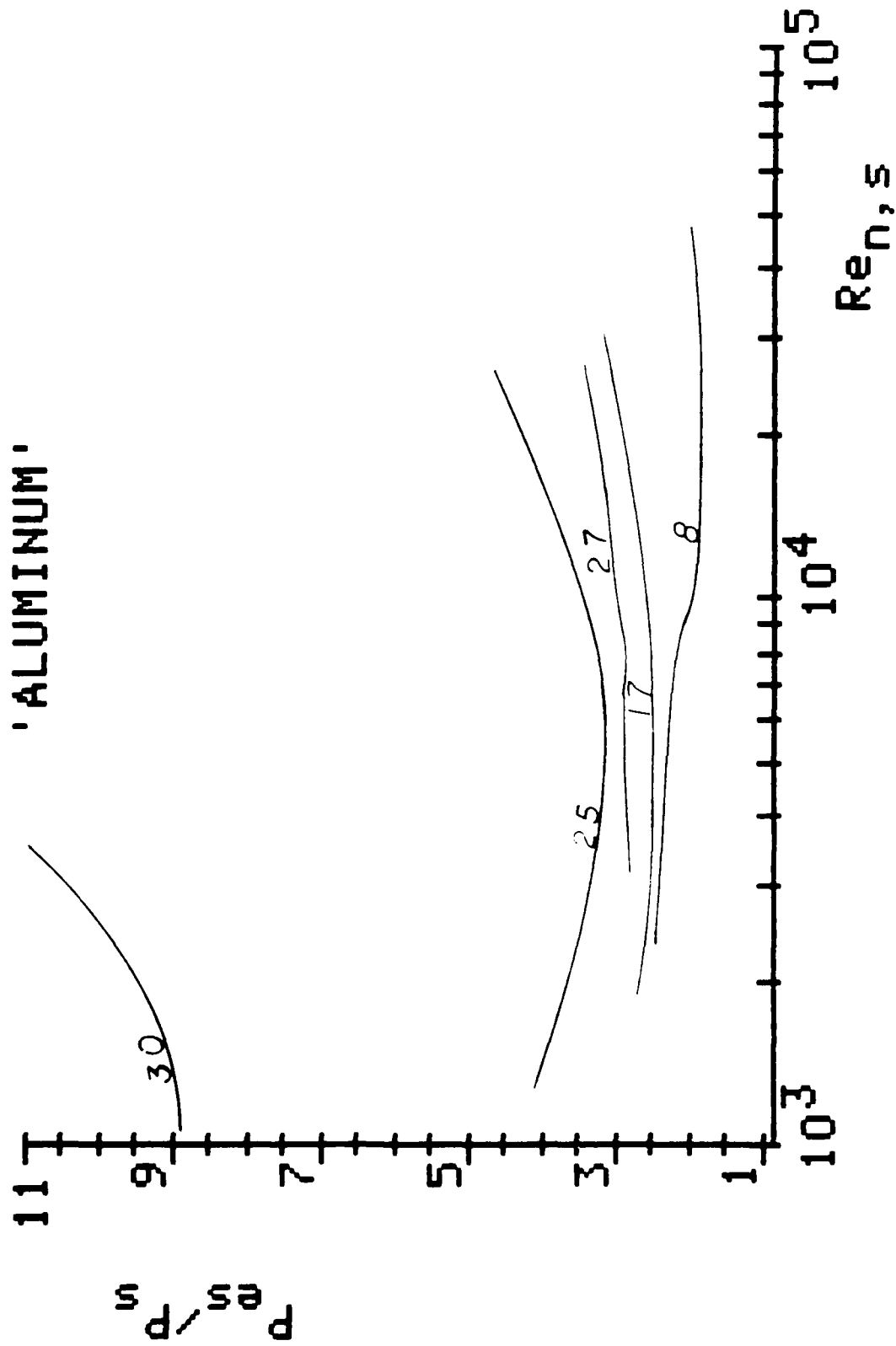Surface 6.2 vs. Smooth Surface Temperature Rise
for Case g.

V.   COMPARISON RESULTS

Table III shows the ranking of the surfaces based on case c by heat exchanger material and surface type in order of decreasing performance within each surface type. Ranking of the best surface for each material, with the surface plate spacing in parentheses, is shown in Table IV. Using aluminum as the "base" surface material, the rankings within each material is shown in Table V of the best aluminum surfaces. Overall ranking of all surfaces considered is shown in Table VI. Because of the proximity of some of the performance curves to each other and curve crossovers the rankings of some surfaces is subjective.

TABLE III: RANKING BY SURFACE TYPE

Surface Type	Stainless Steel	Surface Number Mild Steel	Aluminum	Copper
Plain Plate - Fin	8	8	8	8
	6	6	6	6
	4	4	4	4
	7	7	7	7
	5	5	5	5
	1	1	1	1
	2	2	3	3
	3	3	2	2
Louvered Plate - Fin	17	17	17	17
	15	16	16	16
	19	18	18	19
	16	15	19	18
	18	19	15	15
	20	20	20	20
	22	21	22	21
	21	22	21	22
	14	14	14	14
	13	13	13	13
	10	10	10	10
	12	12	12	12
	11	9	9	11
	9	11	11	9
Strip - Fin Plate - Fin	23	25	25	25
	25	23	23	23
	24	24	24	24
Wavy - Fin Plate - Fin	27	27	27	27
	26	26	26	26
Pin - Fin Plate - Fin	29	29	30	30
	28	28	29	29
	31	30	31	31
	30	31	28	28
	32	32	32	32

TABLE IV: RANKING OF BEST SURFACES

Surface Number

Stainless Steel	Mild Steel	Aluminum	Copper
17 (.250 in)	27 (.413 in)	27 (.413 in)	27 (.413 in)
8 (.250 in)	17 (.250 in)	25 (.414 in)	25 (.414 in)
27 (.413 in)	8 (.250 in)	17 (.250 in)	17 (.250 in)
23 (.250 in)	23 (.250 in)	8 (.250 in)	8 (.250 in)
29 (.398 in)	29 (.398 in)	30 (.750 in)	30 (.750 in)

TABLE V: RANKING BY ALUMINUM "BASE" SURFACE

Surface Number

Stainless Steel	Mild Steel	Aluminum	Copper
17 (.250 in)	27 (.413 in)	27 (.413 in)	27 (.413 in)
8 (.250 in)	17 (.250 in)	25 (.414 in)	25 (.414 in)
27 (.413 in)	8 (.250 in)	17 (.250 in)	17 (.250 in)
25 (.414 in)	25 (.414 in)	8 (.250 in)	8 (.250 in)
30 (.750 in)	30 (.750 in)	30 (.750 in)	30 (.750 in)

TABLE VI: OVERALL SURFACE RANKING

Ranking Number	Stainless Steel	Surface Number Mild Steel	Aluminum	Copper
1	17	27	27	27
2	15	17	25	25
3	19	16	17	17
4	16	8	16	16
5	8	18	18	19
6	27	15	19	18
7	18	19	8	15
8	23	25	15	26
9	20	23	23	8
10	22	20	26	23
11	21	21	20	20
12	25	22	22	24
13	14	26	21	21
14	13	14	24	22
15	29	13	14	30
16	28	29	13	14
17	26	10	30	13
18	10	6	29	29
19	12	28	10	10
20	11	12	6	6
21	6	9	12	12
22	9	30	9	11
23	31	24	11	31
24	4	4	31	28
25	30	31	28	9
26	24	11	4	4
27	7	7	7	7
28	5	5	5	5
29	32	32	32	32
30	1	1	1	1
31	2	2	3	3
32	3	3	2	2

VI. CONCLUSIONS

Using basic heat transfer, friction, and geometric relationships for heat exchanger surfaces, performance parameters can be developed to relate heat transfer, required pumping power and heat exchanger size. These parameters can be used to determine the relative performance of one surface type to another of the same or different materials. The performance parameters need to be modified for the desired comparison based upon the characteristic dimensions of the surface. Cases a through d use volume and cases e through g use length as the characteristic dimensions. Other items to consider when comparing surfaces are what is the desired result, i.e. a reduction in total volume or a reduction in length, and what parameters are to remain constant between the surfaces - - flow rate, pumping power, heat transfer, frontal area, etc.

Case c provides the best way to compare surfaces. By keeping the pumping power and heat transfer constant, case c will indicate which surface will give the smallest heat exchanger for a given flow rate to do the job. It does not indicate however, that one surface is better than another for all applications. Different materials are better than others depending upon the application. Because of different plate spacings and fin thicknesses, surfaces may switch relative positions between materials. Refering to Tables III and IV, in general, as thermal conductivity decreases,

surfaces with smaller plate spacings become the better surfaces. For stainless steel surface number 17, louvered plate - fin surface 1/4 (b) - 11.1, is the best while for mild steel, aluminum, and copper, surface number 27, wavy - fin plate - fin surface 17.8 - 3/8W is the best of the surfaces compared.

BIBLIOGRAPHY

1. Bergles, A. E., A. R. Blumenkrantz, and J. Taborek; "Performance Evaluation Criteria fo Enhanced Heat Transfer Surfaces"; Paper FC6.3 for Fifth International Heat Transfer Conference (1974).

2. Soland, J. G., W. M. Mack, and W. M. Rohsenow; "Performance Ranking of Plate - Fin Heat Exchanger Surfaces"; Journal of Heat Transfer; (1978).

3. Kays, W. M., and A. L. London; Compact Heat Exchangers; Second Edition, McGraw - Hill Book Co., New York, New York (1964).

4. Rohsenow, W. M., and H. Choi; Heat, Mass, and Momentum Transfer; Prentice - Hall Inc., Englewood Cliffs, New Jersey, (1961).

5. Webb, R. L.; "Compact Heat Exchangers"; Heat Transfer Design Handbook; Hemisphere Publishing Corporation, New York, New York, (1986).

6. Webb, R. L.; "Performance Evaluation Criteria for Use of Enhanced Heat Transfer Surfaces in Heat Exchanger Design"; International Journal of Heat and Mass Transfer, (April 1981).

7. Webb, R. L., and E. R. G. Eckert; "Application of Rough Surfaces to Heat Exchanger Design"; International Journal of Heat and Mass Transfer, (September 1972).

8. LaHaye, P. G., F. J. Neugebauer, and R. K. Sakhuja; "A Generalized Prediction of Heat Transfer Surface Performance and Exchanger Optimization"; ASME Paper No. 72-WA/HT-55, (1972).

9. Moody, L. F.; "Friction Factors for Pipe Flow"; ASME Transactions, (November 1944).

10. Dipprey, D. F., and R. H. Sabersky; "Heat and Momentum Transfer in Smooth and Rough Tubes at Various Prandtl Numbers"; International Journal of Heat and Mass Transfer, (May 1963).

11. Cox, B., and P. A. Jallock; "Methods for Evaluating the Performance of Compact Heat Transfer Surfaces"; ASME Paper No. 72-WA/HT-56, (1972).

END

FILMED

MARCH, 1988

DTIC